

# RAPIDLY CONVERGENT «SUPERRESOLVING» DIRECTION-OF-ARRIVAL ESTIMATION OF NOISE RADIATION SOURCES IN ADAPTIVE ARRAYS

D. I. LEKHOVYTSKIY, YA. S. SHIFRIN

The paper summarizes and develops the results obtained by the authors in [11, 33, 49, 50]. We compare the efficiencies of some “superresolving” methods for estimation of a spatial spectrum of Gaussian noise in an antenna array for the case of a finite-size sample in maximum likelihood estimates of their correlation matrices. The comparison is based on an analysis of exact and empirical random parameters distribution laws that determine the methods resolution by statistical and non-statistical criteria. Significant differences in these laws are shown owing to which conclusions about comparative merits of different methods, based on their asymptotic properties analysis, can change to opposite ones under conditions of small samples. Causes of the difference and the possibilities following from their analysis to improve the convergence rate of adaptive methods for noise sources direction-of-arrival estimation are studied.

*Keywords:* direction-of-arrival estimation, «superresolving» space-time spectral analysis, convergence rate, statistical analysis, resolution, finite sample, adaptive lattice filter.

## I. INTRODUCTION AND STATEMENT OF THE PROBLEM

Practical needs for “super-Rayleigh” noise radiation sources resolution and heightening their angular coordinates measurements accuracy have stimulated the development of a great amount of “superresolving” methods of direction of arrival (DoA) estimation in antenna arrays (AA) [1 – 19, etc]. **Yacov D. Shirman** was first who established the “superresolution” fundamental possibility, sense and extreme performance for different applications [20, 21, 34, 35]. An important role in the development of this line of investigation was played by works of J.P. Burg [24] and J. Capon [36]. A flow of publications on this topic including those of review nature, that then followed, goes far beyond the works referred to in this paper.

Merits of the “superresolving” methods have been provided by the processing optimization (by these or those criteria) based on **statistical characteristics** of AA output signals (multivariate probability density functions). Under typical in practice conditions of parametric *a priori* uncertainty, in synthesized algorithms, instead of *a priori* unknown true parameters, these or those their **estimates** obtained by **finite-size** training samples are used. Stipulated by this **randomness** of the estimates entails randomness of parameters characterizing efficiencies of methods used. Their statistically correct comparison therefore has to be based on an analysis of **distribution laws** of relevant random parameters.

Great attention in the literature is paid to the statistical investigations of “superresolving” methods of space-time spectral analysis (ST SA) [1 – 16, 22, 26, etc] including those for solving problems of point noise sources direction finding in AA. Nevertheless, due to a lot of the methods, problems solved with them, and criteria used, the investigations can not be considered as completed. As a development of [15 – 19], in the paper, **exact** or **empirical** (by simulation results) distribution laws are analyzed for spectral functions (SF) of some known ST SA methods given

a finite size sample in the maximum likelihood (ML) estimate of the correlation matrix (CM) of Gaussian noise at AA outputs.

Beside of self-importance, the analysis allows substantiating the simple modifications of considered methods which significantly improve their statistical properties [33].

The paper is organized as follows. Initial models and assumptions are formulated in Section II. Potentialities of Gaussian noisy (in time) quasi-harmonic (in space) signals resolution-detection by means of optimal (by the **Neyman-Pearson** criterion) processing under hypothetical conditions of full *a priori* definiteness are considered in Section III. In Section IV, after the technique is briefly described, exact probability density functions (pdf) of random SFs are presented for some space-time spectral analysis methods given different training sample (herein-after termed sample) sizes in ML estimates of CM. Their resolutions on this basis are compared by statistical (Section V) and non-statistical (Section VI) criteria. Reasons of the difference and following from them ways to improve statistical properties of considered ST SA methods are discussed in Section VII. In Section VIII, new kinds of “superresolving” ST SA methods being highly efficient under conditions of small-size samples are substantiated.

## II. INITIAL RELATIONSHIPS, MODELS AND ASSUMPTIONS

A. Random spectral functions (SF)  $\hat{S}(\alpha) = S(\alpha, \hat{\Psi})$  of considered ST SA methods look like

$$\hat{S}_1(\alpha) = (\mathbf{x}^*(\alpha) \cdot \Psi \cdot \mathbf{x}(\alpha))^{-1}, \quad (MV)$$

$$\hat{S}_2(\alpha) = \omega_{mm} \cdot |\mathbf{e}_m^* \cdot \Psi \cdot \mathbf{x}(\alpha)|^{-2}, \quad m \in 1, M, \quad (LP) \quad (1)$$

$$\hat{S}_3(\alpha) = \frac{\omega_{mm} \cdot \mathbf{x}^*(\alpha) \cdot \Psi \cdot \mathbf{x}(\alpha)}{|\mathbf{e}_m^* \cdot \Psi \cdot \mathbf{x}(\alpha)|^2}, \quad m \in 1, M, \quad (MCA)$$

$$\hat{S}_4(\alpha) = \frac{\mathbf{x}^*(\alpha) \cdot \Psi \cdot \mathbf{x}(\alpha)}{\mathbf{x}^*(\alpha) \cdot \Psi^2 \cdot \mathbf{x}(\alpha)}, \quad (BL)$$

$$\hat{S}_5(\alpha) = (\mathbf{x}^*(\alpha) \cdot \Psi^2 \cdot \mathbf{x}(\alpha))^{-1}. \quad (TN)$$

The SF  $\hat{S}_1(\alpha)$  corresponds to **Capon's** “Minimum Variance” (**MV**) method [1–6, 14, 22, 25];  $\hat{S}_2(\alpha)$  to Burg's “Linear Prediction” (**LP**) method [1, 2, 6, 24, 27];  $\hat{S}_3(\alpha)$  to one of the “Modified **Capon's** Algorithms” (**MCA**) variants [16–19];  $\hat{S}_4(\alpha)$  to Borgiotti-Lagunas's method (**BL**) [3, 6],  $\hat{S}_5(\alpha)$  to the “Thermal Noise (**TN**)” one [6, 14, 27].

In all the SFs,  $\mathbf{x}(\alpha) = \{x_\ell(\alpha)\}_{\ell=1}^M$  is the non-random  $M$ -variate **steering** vector (in  $\alpha$ -direction) subject to  $M$  receive **AA** elements (modules) spacing and performance. In particular, for a linear uniform **AA** (**LUAA**) consisting of identical isotropic elements

$$\mathbf{x}(\alpha) = \left\{ \exp(j \cdot (\ell - (M+1)/2) \cdot \alpha) \right\}_{\ell=1}^M, \quad (2)$$

$$\alpha = 2 \cdot \pi \cdot d \cdot \sin \theta / \lambda,$$

where  $\theta$  is the direction of search counted from the **AA** normal;  $d$  is the distance between adjacent **AA** elements;  $\lambda$  is the wavelength.

The  $\mathbf{e}_m$  in (1) denotes the  $m$ th ( $m \in 1, M$ ) column of a  $M \times M$  identity matrix  $\mathbf{I}_M$  (the  $M$ -variate vector with a single non-zero ( $m$ th) element equal to unit); (\*) is a sign of Hermitian conjugation.

**B.** Statistical properties of SFs (1) are defined by the properties of the random  $M \times M$  matrix

$$\hat{\Psi} = \left\{ \hat{\omega}_{ij} \right\}_{i,j=1}^M = \hat{\Phi}^{-1}, \quad (3)$$

being inverse to the used estimate  $\hat{\Phi} = \left\{ \hat{\varphi}_{ij} \right\}_{i,j=1}^M$  of the *a priori* unknown spatial **CM**

$$\Phi = \left\{ \varphi_{ij} \right\}_{i,j=1}^M = \overline{\mathbf{y}_\ell \cdot \mathbf{y}_\ell^*}, \quad \ell \in 1, L \quad (4)$$

of  $M$ -variate random vectors  $\mathbf{y}_\ell = \left\{ y_i^{(\ell)} \right\}_{i=1}^M$  of complex amplitudes of **AA** output signals at the discrete  $\ell$ th ( $\ell \in 1, N$ ) time moment.

As usually [3–14], assume these vectors to be normal (Gaussian), interdependent, with a zero mean and the same **CM** (4):

$$\mathbf{y}_\ell \sim CN(0, \Phi), \quad \overline{\mathbf{y}_\ell} = 0, \quad \overline{\mathbf{y}_\ell \cdot \mathbf{y}_m^*} = \Phi \cdot \delta_{\ell m}, \quad \ell, m \in 1, N. \quad (5)$$

Here,  $\delta_{\ell m}$  is the **Kroneker** delta; the bar, like in (4), symbolizes the statistical averaging.

Formed by  $N \geq M$ -size sample  $\mathbf{Y} = \left\{ \mathbf{y}_\ell \right\}_{\ell=1}^N$ , the random matrix

$$\hat{\Phi} = \left\{ \hat{\varphi}_{ij} \right\}_{i,j=1}^M = \frac{1}{N} \cdot \mathbf{Y} \cdot \mathbf{Y}^* = \frac{1}{N} \cdot \mathbf{A}, \quad (6)$$

under conditions (5), as is well known, is the **ML** estimate of unknown **CM** (4). Namely its use in (3) is implied below when analyzing statistical properties of methods (1). The analysis is essentially based on the known property of estimate (6) related to that the random  $M \times M$  matrix that defines it

$$\mathbf{A} = \left\{ a_{ij} \right\}_{i,j=1}^M = \mathbf{Y} \cdot \mathbf{Y}^* = \sum_{\ell=1}^N \mathbf{y}_\ell \cdot \mathbf{y}_\ell^*, \quad (7)$$

given  $N \geq M$  has the **complex Wishart** distribution [23] with the **pdf**

$$p(\mathbf{A}; \Phi, \delta) = I^{-1}(\Phi) \cdot |\mathbf{A}|^\delta \cdot \exp\left\{-tr(\Phi^{-1} \cdot \mathbf{A})\right\}, \quad (8)$$

$$\delta = N - M \geq 0.$$

Here,  $|\mathbf{C}|$  and  $tr(\mathbf{C})$  are the matrix  $\mathbf{C}$  determinant and trace;

$$I(\Phi) = \pi^{M \cdot (M-1)/2} \cdot |\Phi|^{M+\delta} \cdot \prod_{i=1}^M \Gamma(M + \delta + 1 - i)$$

is the normalizing multiplier;  $\Gamma(x)$  the Gamma function [31] that for integer  $x = m \geq 1$  is equal to  $\Gamma(m) = (m-1)!$ .

The **pdf** parameters in (8) are  $\delta = N - M \geq 0$  (**effective sample size**) and true **CM**  $\Phi$  (4), what is reflected in the designation  $p(\mathbf{A}; \Phi, \delta)$ .

**C.** We suppose that for the true **CM** admissible is the presentation [4–14, 19]

$$\mathbf{I}_M + \sum_{i=1}^n h_i \cdot \mathbf{x}(\beta_i) \cdot \mathbf{x}^*(\beta_i) = \mathbf{I}_M + \mathbf{G} \cdot \mathbf{h} \cdot \mathbf{G}^*, \quad (9)$$

$$\mathbf{G} = \left\{ \mathbf{x}(\beta_i) \right\}_{i=1}^n, \quad \mathbf{x}(\beta_i) = \left\{ x_\ell(\beta_i) \right\}_{\ell=1}^M, \quad \mathbf{h} = \text{diag}\{h_i\}_{i=1}^n.$$

It implies **interdependence** of  $M$  receive elements self-noise with the **same** variance (power) (assumed to be unit) and **noncorrelatedness** of radiations of  $n$  external sources with relative (with respect to a level of the elements self-noise) intensities (**SNR**)  $h_i$  ( $i \in 1, n$ ). The  $M$ -variate vector-columns  $\mathbf{x}(\beta_i)$  of  $M \times n$  matrix  $\mathbf{G}$  (9) describe the aperture amplitude-phase distribution of radiations from the  $\beta_i$ -directions ( $i \in 1, n$ ). For **LUAA**, in particular, they look like (see (2))

$$\mathbf{x}(\beta_i) = \left\{ \exp(j \cdot (\ell - (M+1)/2) \cdot \beta_i) \right\}_{\ell=1}^M, \quad (10)$$

$$\beta_i = 2 \cdot \pi \cdot d \cdot \sin \theta_i / \lambda, \quad i \in 1, n,$$

where  $\theta_i$  is the direction to the  $i$ th source counted from the **AA** normal.

Matrix  $\Psi$  being inverse to  $\Phi$  (9) equals

$$\Psi = \left\{ \omega_{ij} \right\}_{i,j=1}^M = \Phi^{-1} = \mathbf{I}_M - \mathbf{G} \cdot (\mathbf{h}^{-1} + \mathbf{G}^* \cdot \mathbf{G})^{-1} \cdot \mathbf{G}^*. \quad (11)$$

The latter equality in (5), as well as (9) and (10) reflect a **noisy in time** and **quasi-harmonic in space** character of point sources signals, and, for brevity, hereinafter they are therefore termed **noisy quasi-harmonic** signals. Besides, by virtue of unambiguous relation between true ( $\theta$ )- and “generalized” ( $\alpha, \beta$ )-directions, the **latter** ones only, without reserve and quotes, are used below.

### III. POTENTIALITIES OF NOISY QUASI-HARMONIC SIGNALS RESOLUTION-DETECTION

**A.** **Shirman's** statistical theory developed in works [20, 21, 34] treats various kinds and criteria of resolution. Here, concepts of the quasi-complete **resolution-detection** theory are used. According to it,  $n$  signals in noise are considered as resolved if the **statistical** characteristics of **detection** (conditional false

alarm probabilities (**FAP**)  $F$  and proper detection probability (**PDP**)  $D$  of each of them **by turns** playing a role of useful signal in the presence of the rest  $(n-1)$  signals playing a role of **interfering** ones, remain **not worse** than an admissible limit.<sup>1</sup>

In such a statement, a procedure of spatial resolution is reduced to testing the hypotheses: either  $H_1$  about the **presence** or  $H_0$  about the **absence** of a source in successively or simultaneously tested **signal** directions  $\alpha$  of sector  $(\alpha_b, \alpha_e)$  chosen. The resolution-detection potentialities are provided by the **optimal** processing of received realization under hypothetical conditions of **full a priori definiteness**.

**B.** As applied to the models of Section II, the latter means a knowledge of  $\alpha$ -dependent **CMs**  $\Phi_1$  and  $\Phi_0$  of vectors  $\mathbf{y}_\ell$  (5) by hypotheses  $H_1$  and  $H_0$ . They are related to **CM**  $\Phi$  (9) by the equalities

$$\Phi = \begin{cases} \Phi_0 = \Psi_0^{-1}, & \alpha \neq \beta_\ell, \\ \Phi_1 = \Phi_0 + h_\ell \cdot \mathbf{x}(\beta_\ell) \cdot \mathbf{x}^*(\beta_\ell), & \alpha = \beta_\ell, \end{cases} \ell \in 1, n. \quad (12)$$

In this case, the optimal (by the **Neyman-Pearson** criterion) processing of the  $K$ -variate realization of input process  $\mathbf{Y} = \{\mathbf{y}_\ell\}_{\ell=1}^K$  is reduced to **formation of the statistic** [18, 34]

$$\xi(\alpha) = \mathbf{r}_0^*(\alpha) \cdot \hat{\Phi} \cdot \mathbf{r}_0(\alpha) = \frac{1}{K} \cdot z(\alpha), \quad (13)$$

$$z(\alpha) = \mathbf{r}_0^*(\alpha) \cdot \mathbf{A} \cdot \mathbf{r}_0(\alpha), \quad \mathbf{r}_0(\alpha) = \Psi_0 \cdot \mathbf{x}(\alpha),$$

and to its comparison with the threshold  $v_0(\alpha)$  providing the specified **FAP**

$$F = \int_{v_0(\alpha)}^{\infty} p_{\xi_0}(x) dx = \int_{K \cdot v_0(\alpha)}^{\infty} p_{z_0}(x) dx. \quad (14)$$

Here,  $p_{\xi_0}(x)$  and  $p_{z_0}(x)$  denote **pdfs** of the statistics  $\xi(\alpha)$  and  $z(\alpha)$  under **hypothesis**  $H = H_0$  of the **absence** of sources in the direction under analysis.

Using (8) with  $M=1$  and  $N=K$  and taking into account (12), it is easy to make sure [19] that  $p_{z_0}(x) = p_z(x, \sigma_0^2)$  where

$$p_z(x, \sigma^2) = \frac{1}{\sigma^2 \cdot (K-1)!} \cdot \left(\frac{x}{\sigma^2}\right)^{K-1} \cdot \exp\left\{-\frac{x}{\sigma^2}\right\} \quad (15)$$

is **pdf** of **Gamma-distribution** with the integer shape parameter  $K$  (**Erlang's** distribution [30]) and the scale parameter

$$\sigma^2(\alpha) = \overline{\xi(\alpha)} = \mathbf{r}_0^*(\alpha) \cdot \Phi \cdot \mathbf{r}_0(\alpha) = \begin{cases} \sigma_0^2(\alpha) = \mathbf{x}^*(\alpha) \cdot \Psi_0 \cdot \mathbf{x}(\alpha), & \alpha \neq \beta_\ell, \\ \sigma_1^2(\alpha) = \sigma_0^2 \cdot (1 + \mu_\ell), & \alpha = \beta_\ell, \end{cases} \ell \in 1, n, \quad (16)$$

$$\mu_\ell = \frac{\sigma_1^2 - \sigma_0^2}{\sigma_0^2} = h_\ell \cdot \mathbf{x}^*(\beta_\ell) \cdot \Psi_0 \cdot \mathbf{x}(\beta_\ell), \quad \alpha = \beta_\ell, \ell \in 1, n. \quad (17)$$

It follows from (14) – (16) that the required threshold level equals

<sup>1</sup> Works [2, 4, 7 – 14 etc.], wherein resolution is linked to an angular coordinates estimation accuracy (with a degree of errors proximity to the **Cramer-Rao** bound), from positions of the theory of [20, 21, 34] concern quasi-complete **resolution-measurement**.

$$v_0(\alpha) = x_0 \cdot \sigma_0^2(\alpha) / K \quad (18)$$

where  $x_0$  is a root of the equation  $F = \varphi(x_0)$ , whereas

$$\varphi(x) = \int_x^{\infty} p_z(x, 1) dx = e^{-x} \cdot \sum_{i=0}^{K-1} x^i / i! \quad (19)$$

is the “survival function” [30] of **Erlang's** distribution with  $\sigma^2 = 1$ . Herewith **PDP** of the signal (from the direction of search  $\alpha$ ) given  $\alpha = \beta_\ell$

$$D = D(\mu_\ell) = \int_{K \cdot v_0(\alpha)}^{\infty} p_z(x, \sigma_1^2) dx = \varphi\left(\frac{x_0}{1 + \mu_\ell}\right), \quad \ell \in 1, n \quad (20)$$

fully depends on the **detection** parameter  $\mu_\ell$  (17). It has an evident sense of “optimal” signal to interference (a mixture of interfering signals from the  $\beta_i \neq \alpha$  directions and receive channels noise) power ratio (**OSIR**) **after** the optimal processing. It is convenient to write it down as

$$\mu_\ell = q_\ell \cdot k_e, \quad q_\ell = r \cdot h_\ell, \quad \ell \in 1, n, \quad (21)$$

$$k_e = \mathbf{x}^*(\beta_\ell) \cdot \Psi_0 \cdot \mathbf{x}(\beta_\ell) / r, \quad r = \mathbf{x}^*(\beta_\ell) \cdot \mathbf{x}(\beta_\ell),$$

where  $q_\ell$  is the **OSIR** in the absence of “interfering” signals (in the presence of self-noise solely) to be henceforth termed **OSNR** in order to emphasize its dissimilarity from **SNR**  $h_\ell$  in the **AA** elements;  $k_e \leq 1$  is the “**useful**” signal energy utilization factor [20] characterizing the loss due to the presence of “**interfering**” signals.

In particular, for **LUAA** given  $n=2$  and  $\alpha = \beta_i$  when, by virtue of (9) – (12),

$$\mathbf{G} = \mathbf{x}(\beta_2), \quad r = M, \quad \Psi_0 = \mathbf{I}_M - \frac{h_2}{1 + q_2} \cdot \mathbf{x}(\beta_2) \cdot \mathbf{x}^*(\beta_2) \quad (22)$$

from (21) obtain [18 – 21, 34]

$$\mu_1 = q_1 \cdot k_e, \quad k_e = 1 - \frac{q_2}{1 + q_2} \cdot |\rho|^2, \quad (23)$$

$$q_i = M \cdot h_i, \quad i = 1, 2.$$

Here,

$$\rho = \mathbf{x}^*(\beta_1) \cdot \mathbf{x}(\beta_2) / r \approx \sin(\pi \cdot \Delta) / (\pi \cdot \Delta) \quad (24)$$

is the spatial correlation factor of “useful” and “interfering” signals subject to the **relative** angular distance between them

$$\Delta = (\beta_2 - \beta_1) / \Delta_0, \quad \Delta_0 = 2 \cdot \pi / M; \quad (25)$$

$\Delta_0$  is the **first nulls** radiation pattern (**RP**) half-width of the synphase  $M$ -element **LUAA**.

The approximate equality in (24) is valid under conditions of  $M \gg 1$  and  $\Delta \leq 1$  to be of key interest for the later discussion.

**C.** Fig. 1a shows families of the dependences  $D = D(\mu)$ , with  $\mu = q \cdot k_e$  and  $q = q_1$ , accounted by (20), (19) for different values of  $F$  and sizes  $K$  of the analyzed input process realization  $\mathbf{Y} = \{\mathbf{y}_\ell\}_{\ell=1}^K$ . Fig. 1b shows dependences  $k_e(\Delta)$  (23) – (25) for a set of **OSNR** values  $q_M = q_2$  of “interfering” signal. They allow defining the statistical **detection** characteristics  $(F, D)$  of the signal with **OSNR**  $q$  versus the angular distance  $\Delta \leq 1$  between them and, hence, the possibilities of their angular **resolution-detection**.

Let, e.g.,  $q = 20$  (13 dB),  $K = 5$ , and **PDP** have to be not less than  $D \geq D_{allow} = 0.5$  for **FAP**  $F = 10^{-6}$ . As follows from Fig. 1a,  $\mu \geq 4$  and hence  $k_e \geq 0.2$  (-7 dB) are required for this. According to Fig. 1b, this  $k_e$  value is provided for  $\Delta \geq 0.19$  if  $q_M = 10$  dB, and for  $\Delta \geq 0.22$  if  $q_M = 15$  dB. When  $\Delta \geq 0.23$ , it is provided even if  $q_M \rightarrow \infty$ . The corresponding lower bound  $\Delta = \Delta_{min}$ , as is seen from the given examples and was shown as early as in [20], can be less than the **Rayleigh** limit  $\Delta = \Delta_R \approx 1$ . This bound is provided solely under hypothetic conditions of full *a priori* definiteness with optimal processing (13) of the signals described in Section II and therefore characterizes their resolution-detection **potentialities**.

The “**super-Rayleigh**” resolution is “purchased” at the expense of the **increase**  $\mu/q = k_e^{-1}$  times in the signal threshold power. However, under optimal processing (13), power loss (21), (23) is **minimum**, or, what is the equivalent, the power is used for **resolution** as much effectively as possible. For example, in a test scenario of two ( $n = 2$ ) equipotent **LUAA** signals,  $\Delta_{min}$  is **inversely** proportional to  $\sqrt{q}$  given “small”  $K$ , and to  $q$  given the “large”  $K$ . A boundary between the “small” and “large”  $K$  is subject to  $D$  and  $F$ . It can be shown, in particular, that for  $D = 0.5$  and  $F = 10^{-6}$  [18, 19],

$$\Delta_{min} = \begin{cases} \approx 1/\sqrt{q} & \text{for } K \leq 5, \\ \leq 0.577/q & \text{for } K \geq 35. \end{cases} \quad (26)$$

**D.** The processing under real conditions of *a priori* uncertainty is inevitably related to an **additional** signal loss and (or) **aggravation of requirements** to the sample size (observation interval). These loss and requirements being a “pass” for these or those methods to the work under corresponding conditions are defined by **distribution laws** of statistics formed by the methods. Below, a role of the statistics is played by random **SFs** of methods (1), wherein instead of unknown **CMs** (9), (11) their **ML** estimates (6), (3) are used.

#### IV. DISTRIBUTION LAWS OF SPECTRAL FUNCTIONS “AT POINT”

**A.** In an optimal resolution-detection procedure, statistic (13) at points of analysis  $\alpha \in (\alpha_b, \alpha_e)$  is compared with threshold (18), (19) (**for the moment** (until Section VI) we assume that necessary thresholds can be formed).

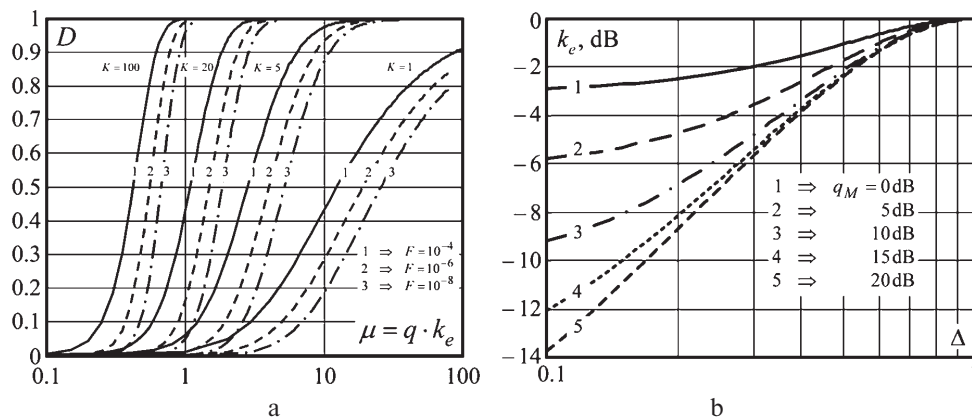


Fig. 1. (a) Dependences  $D = D(\mu)$ . (b) Dependences  $k_e(\Delta)$  (23) – (25) for a set of  $q_2$

The statistical characteristics of the threshold processing of random **SFs**  $\hat{S}(\alpha)$  (1) are defined by distribution laws of their values at these points.

When deriving the laws, assume **ML** estimates (6), (3) to be formed by the  $N \geq M$  sample  $\mathbf{Y} = \{\mathbf{y}_\ell\}_{\ell=1}^N$  of vectors  $\mathbf{y}_\ell$  with properties (5), so matrix **A** (7) has the **Wishart** distribution (8):

$$\mathbf{A} = \mathbf{Y} \cdot \mathbf{Y}^*, p(\mathbf{A}) = p(\mathbf{A}; \Phi, \delta), \delta = N - M \geq 0. \quad (27)$$

Having no possibility to give here complicated and bulky computations, we restrict ourselves by a brief description of a **procedure** and results of **exact** computation of the **pdf** for the first three **SFs** (1) only that are direct subject to matrix  $\hat{\Psi}$ . The **pdfs** of the two latter **SFs** dependent on the **squared** matrix are unknown for the authors. Their empirical distribution laws are obtained below with the help of a mathematical model **pretested with exact** results.

**B.** The essence of the technique is in the following [15]. Let us introduce the  $k \times k$  Hermitian matrix

$$\hat{\mathbf{Q}} = \{\hat{q}_{ij}\}_{i,j=1}^k = \mathbf{Z}^* \cdot \mathbf{A}^{-1} \cdot \mathbf{Z} = N^{-1} \cdot \mathbf{Z}^* \cdot \Psi \cdot \mathbf{Z}, \quad (28)$$

$$\mathbf{Z} = \{\mathbf{z}_i\}_{i=1}^k, \quad k \leq M,$$

where **A** is random matrix (27); **Z** the non-random full column-rank matrix (with  $k \leq M$  linearly independent  $M$ -variate columns  $\mathbf{z}_i, i = 1, k$ ).

It can be shown [47] that the  $k \times k$  matrix

$$\hat{\mathbf{R}} = \{\hat{r}_{ij}\}_{i,j=1}^k = \hat{\mathbf{Q}}^{-1} \quad (29)$$

under conditions of (27) has the **Wishart** distribution

$$p(\hat{\mathbf{R}}) = d^{-1} \cdot |\hat{\mathbf{R}}|^\delta \cdot \exp\{-tr(\Omega \cdot \hat{\mathbf{R}})\}, \quad (30)$$

$$d = \pi^{\frac{k(k-1)}{2}} \cdot |\Omega^{-1}|^{\delta+k} \cdot \prod_{i=1}^k \Gamma(k + \delta - i + 1)$$

with the  $k \times k$  non-random **matrix of parameters**  $\Omega^{-1}$ ,

$$\Omega = \{\Omega_{ij}\}_{i,j=1}^k = \mathbf{Z}^* \cdot \Psi \cdot \mathbf{Z}. \quad (31)$$

Given  $k = M$  and  $\mathbf{Z} = \mathbf{I}_M$ , when  $\Omega = \Psi$ ,  $\Omega^{-1} = \Phi$ ,  $\hat{\mathbf{Q}} = \mathbf{A}^{-1}$  and hence  $\hat{\mathbf{R}} = \mathbf{A}$ , distribution (30) turns into (8).

**C.** Let  $k = 1$  and  $\mathbf{Z} = \mathbf{z}_1 = \mathbf{x}(\alpha)$ . In this case, **matrices** (28) – (30) are transformed into the **scalars**

$$\Omega = S_1^{-1}(\alpha), \quad \Omega^{-1} = S_1(\alpha), \quad d = \delta! \cdot S_1(\alpha)^{\delta+1},$$

$$\hat{\mathbf{Q}} = (N \cdot \hat{S}_1(\alpha))^{-1}, \quad \hat{\mathbf{R}} = N \cdot \hat{S}_1(\alpha),$$

and distribution (30) takes the form

$$p(\hat{R}) = (\delta! \cdot S_1(\alpha))^{-1} \cdot \left( \hat{R}/S_1(\alpha) \right)^\delta \cdot \exp\left\{-\hat{R}/S_1(\alpha)\right\}.$$

The **pdf** of **SF**  $\hat{S}_1(\alpha) = \hat{R}/N$  of **Capon's MV** method therefore equals

$$P_{\hat{S}_1}(x) = \frac{1}{\delta!} \cdot \frac{N}{S_1(\alpha)} \cdot \left( \frac{x \cdot N}{S_1(\alpha)} \right)^\delta \cdot \exp\left\{-\frac{x \cdot N}{S_1(\alpha)}\right\} \quad (32)$$

where  $S_1(\alpha)$  is the “true” value of **SF** (given  $\hat{\Psi} = \Psi$ ).

In this case, the “**normalized**” **SF**, being more convenient for the further analysis,

$$v = \hat{S}(\alpha)/S(\alpha) \quad (33a)$$

with the **pdf**

$$p_v(x) = S(\alpha) \cdot p_{\hat{S}}(S(\alpha) \cdot x), \quad (33b)$$

for the **MV** method equals

$$p_v(x) = p_{v_1}(x) = (\delta!)^{-1} \cdot N \cdot (N \cdot x)^\delta \cdot \exp\{-N \cdot x\}. \quad (34)$$

**Pdfs** (32), (34) were first obtained as early as in [22] and then “re-derived” in [23]. In [19, 28], they were obtained also for **ML** estimates of **persymmetrical CMs** being possible, in particular, in **AAs** with the **central symmetry** in spacing of pairwise identical receive elements (modules) [3, 18]. Discussion on peculiarities related to this **CM** specificity as well as to other ones is a subject for a separate publication.

Let now  $k=2$ , and  $\mathbf{Z} = \{\mathbf{z}_1, \mathbf{z}_2\}$  be the  $M \times 2$  matrix with the columns

$$\mathbf{z}_1 = \mathbf{e}_m, \quad \mathbf{z}_2 = \mathbf{x}(\alpha), \quad m \in 1, M. \quad (35)$$

In this case, **pdf** (30) of the  $2 \times 2$  matrix

$\hat{\mathbf{R}} = \{\hat{r}_{ij}\}_{i,j=1}^2$  equals

$$p(\hat{\mathbf{R}}) = (\pi \cdot \delta! \cdot (\delta+1)!)^{-1} \cdot |\hat{\mathbf{Q}}|^{\delta+2} \cdot |\hat{\mathbf{R}}|^\delta \cdot \exp\{-tr(\hat{\mathbf{Q}} \cdot \hat{\mathbf{R}})\}, \quad (36)$$

$$\hat{\mathbf{Q}} = \mathbf{Z}^* \cdot \Psi \cdot \mathbf{Z},$$

and the first three **SFs** of (1) are related to  $2 \times 2$  matrix  $\hat{\mathbf{Q}}$  (28) elements as

$$\hat{S}_1 = \frac{1}{N \cdot \hat{q}_{22}}, \quad \hat{S}_2 = \frac{\hat{q}_{11}}{N \cdot |\hat{q}_{12}|^2}, \quad \hat{S}_3 = \frac{\hat{q}_{11} \cdot \hat{q}_{22}}{|\hat{q}_{12}|^2} \quad (37)$$

(for the moment, for designation simplicity, argument  $\alpha$  of the **SFs** is omitted).

**D.** Therewith the problem to be solved is reduced to solving two subproblems:

a) to find **pdf** of  $2 \times 2$  matrix  $\hat{\mathbf{Q}}$  (28) via **pdf** (36) of matrix  $\hat{\mathbf{R}}$  (29);

b) to account **pdfs** (37) of matrix  $\hat{\mathbf{Q}}$  elements.

In order for the **first** of them to be solved, it is enough to take into account that Jacobian of transform (29) is equal to  $|\hat{\mathbf{Q}}|^{2k}$  and consequently for  $k=2$

$$p(\hat{\mathbf{Q}}) = |\hat{\mathbf{Q}}|^{\delta+2} \cdot |\hat{\mathbf{Q}}|^{-(\delta+4)} \cdot \frac{\exp\{-tr(\hat{\mathbf{Q}} \cdot \hat{\mathbf{Q}}^{-1})\}}{\pi \cdot \delta! \cdot (\delta+1)!}. \quad (38)$$

The **second** problem is **more challenging**. It requires rather nontrivial transforms, calculations of their Jacobians and integrals containing special functions some of which are reduced to the reference ones [31].

Omitting details, we give the “final” **joint pdfs** of values fully defining sought random **SFs**  $\hat{S}_2$  and  $\hat{S}_3$  (37):

$$p_c(v_2, v_3) = d_{23} \cdot \exp\left\{-\frac{N \cdot v_2}{v_3}\right\} \times \exp\left\{-\frac{N \cdot v_2}{1 + C_3 \cdot v_3}\right\} \cdot L_{\delta+1}\left\{-\frac{N \cdot v_2}{C_3 \cdot v_3 \cdot (1 + C_3 \cdot v_3)}\right\}, \quad (39a)$$

$$d_{23} = \frac{1}{\delta! \cdot C_3 \cdot v_3^2} \cdot N^{\delta+2} \cdot v_2^{\delta+1} \cdot \left(\frac{C_3}{1 + C_3 \cdot v_3}\right)^{\delta+2}.$$

Here,  $L_n(\bullet)$  is the **Laguerre** polynomial of degree  $n$  [31],

$$v_2 = \hat{S}_2/S_2, \quad v_3 = \hat{C}_3/C_3, \quad \hat{C}_3 = \hat{S}_3 - 1 \quad (39b)$$

are the random **SFs** values **normalized** to the “true” ones.

Integrating (39a) over  $v_2$  ( $v_3$ ) from 0 to  $\infty$ , obtain the **pdfs**  $p_v(x)$  of **normalized SFs**  $v = v_3$  ( $v = v_2$ ). The integral over  $v_2$  is written as

$$p_v(x) = p_{v_3}(x) = C^{\delta+1} \cdot (\delta+1) \times \sum_{n=0}^{\delta+1} \frac{a_n}{C^n} \cdot \frac{x^\delta}{(1 + (1+C) \cdot x)^{\delta+2+n}}, \quad (40)$$

$$a_n = \frac{(\delta+1+n)!}{(n!)^2 \cdot (\delta+1-n)!}, \quad C = C_3 = C_3(\alpha) = S_3(\alpha) - 1.$$

Attempts to obtain an explicit expression for the integral

$$p_v(x) = p_{v_2}(x) = \int_0^\infty p_c(x, y) dy \quad (41)$$

failed, the **pdf**  $p_{v_2}(x)$  of the **LP** methods is therefore defined with numerical integration methods.

**E.** The analysis carried out in Section V for estimation of methods (1) resolution by statistical resolution-detection criteria is based on **exact** formulas (34), (40), (41) and **empirical** laws of distribution “at point” of **SFs**  $\hat{S}_4(\alpha)$  and  $\hat{S}_5(\alpha)$  of the **BL** and **TN** methods, obtained with models tested by exact formulas.

## V. COMPARATIVE ANALYSIS OF RESOLUTION BY STATISTICAL RESOLUTION-DETECTION CRITERIA

**A.** Assume a decision on signal detection from the  $\alpha \in (\alpha_b, \alpha_e)$ -direction to be made by results of a **comparison** of the random **SFs**  $\hat{S}(\alpha)$  of methods (1) with the **threshold**  $v(\alpha)$ . Their resolution in this case is subject to **FAP**  $F$  and **PDP**  $D$ :

$$F = \int_{v(\alpha)}^\infty p_{\hat{S}}(x, S_0) dx = \int_{x_0}^\infty p_v(x, S_0) dx,$$

$$D = \int_{v(\alpha)}^\infty p_{\hat{S}}(x, S_C) dx = \int_{x_0/(S_C/S_0)}^\infty p_v(x, S_C) dx, \quad (42)$$

where  $S_0 = S_0(\alpha)$  and  $S_C = S_C(\alpha)$  are the true **SFs**  $S(\alpha)$  at a point of analysis  $\alpha$  in the absence

and presence of a source in the  $\alpha$ -direction;  $x_0 = v(\alpha)/S_0(\alpha)$  is the scalar that shows an excess of the threshold

$$v(\alpha) = x_0 \cdot S_0(\alpha) \quad (43)$$

over a  $S_0(\alpha)$  value providing a specified **FAP**  $F$ . The second equalities in (42) are resulted from (33).

It is easy to show that the ratio  $S_C/S_0 = S_C(\alpha)/S_0(\alpha)$  entering the lower limit of the second integral in (42) for all the methods (1) is the **same**, and in the  $\alpha = \beta_\ell$ -directions ( $\ell \in 1, n$ ) of sources location equals (see (17), (21))

$$\frac{S_C}{S_0} = \frac{S_C(\beta_\ell)}{S_0(\beta_\ell)} = 1 + \mu_\ell, \quad \mu_\ell = q_\ell \cdot k_\ell, \quad \ell \in 1, n \quad (44)$$

i.e. it is defined by the same **OSIR**  $\mu_\ell$  as that at the optimal processing under conditions of full *a priori* definiteness (Section III).

**B.** Let us begin from the analysis of **Capon's** method resolution. As follows from the comparison of (34) with (15), for this method, according to (42),

$$F = f_\delta(N \cdot x_0), \quad D = f_\delta\left(\frac{N \cdot x_0}{1 + \mu_\ell}\right), \quad \ell \in 1, n \quad (45)$$

where  $f_\delta(x)$  is the “survival” function of **Erlang's** distribution with the unit scale parameter but unlike (19) with the shape parameter  $\delta + 1$ .

In combination with (20), this means that **Capon's** method under conditions of (6), (3) theoretically provides **exactly the same** statistical performance of resolution-detection as **optimal** processing (13) of the  $K$ -variate input realization  $\mathbf{Y} = \{\mathbf{y}_i\}_{i=1}^K$  if the sample size  $N$  in **ML** estimate (27) satisfies the condition  $\delta = K - 1 = N - M$ , i.e. when

$$N = K + \varepsilon, \quad \varepsilon = M - 1. \quad (46)$$

The  $\varepsilon$  value defines a “payment” for the *a priori* lack of knowledge of **CM**  $\Phi$  (4), which is required when using **Capon's** method on the basis of **ML** estimates (6), (7), (27). In particular, the  $K$  value in Fig. 1a should be increased by  $\varepsilon$  in order to define this method statistical performance in **LUAA** for  $n = 2$  and  $\alpha = \beta_\ell$  ( $\ell \in 1, n$ ).

**C.** The corresponding “payment” of other methods (1) can be **significantly higher**. We will illustrate this first on an example of **MCA** with **SF**  $\hat{C}(\alpha) = \hat{S}(\alpha) - 1$  with **pdf** (40) and the true values  $C(\alpha) = C_0$  and  $C(\alpha) = C_1$  given  $\alpha \neq \beta_\ell$  and  $\alpha = \beta_\ell$  ( $\ell \in 1, n$ ) respectively.

It can be shown that in this case the threshold constant  $x_0$  in (43) is the root of the equation

$$F = \left(\frac{C_0}{1 + C_0}\right)^{\delta+1} \cdot (\delta+1) \cdot \sum_{n=0}^{\delta+1} \frac{a_n}{C_0^n} \cdot I_n(x_0, C_0), \quad (47)$$

and **PDP** of the source signal acting from the  $\alpha = \beta_\ell$ -direction ( $\ell \in 1, n$ ) equals

$$D = (C_1/(1 + C_1))^{\delta+1} \cdot (\delta+1) \times \sum_{n=0}^{\delta+1} a_n \cdot I_n(x_0/(1 + \mu_\ell), C_1), \quad C_1 = C_0/(1 + \mu_\ell), \quad (48)$$

where  $I_n(x, c)$  denotes the integral [31]

$$I_n(x, c) = \int_0^{z(x, c)} t^n \cdot (1-t)^\delta dt = z^{n+1}(x, c) \times \sum_{k=0}^{\delta} (-1)^k \cdot \binom{k}{\delta} \cdot \frac{z^k(x, c)}{n+1+k}, \quad z(x, c) = \frac{1}{1+(1+c) \cdot x}, \quad (49)$$

and  $\binom{m}{n}$  denotes the number of combinations by  $m$  of  $n$ .

Consider first a “small” effective sample size  $\delta$  scenario when

$$(\delta+1) \cdot (\delta+2) < C_0, \quad \delta = N - M \quad (50)$$

As the analysis shows, in this case, a decisive contribution to sums in (47), (48) is made by the **first summands only**, so that

$$F \approx \left(\frac{C_0}{1 + C_0}\right)^{\delta+1} \cdot \frac{\delta+1}{1+(1+C_0) \cdot x_0}, \quad (51)$$

$$D \approx \left(\frac{(1+C_0) \cdot (1+\mu_\ell)}{1+C_0 \cdot (1+\mu_\ell)}\right)^{\delta+1} \cdot F.$$

It follows from the first equality that under conditions of (50) when  $\delta \ll C_0$

$$x_0 \approx \frac{\delta+1}{1+C_0} \cdot F^{-1}. \quad (52)$$

For the probabilities  $F < 10^{-3}$  being of primary interest, this  $x_0$  value can significantly exceed  $x_0$  in (45) for **Capon's** method what demonstrates that distribution (40) has essentially “**heavier tails**” than distribution (34).

It can be seen from the second equation in (51) that for small **OSIR** values  $\mu_\ell < 1$ ,  $D \approx F$  what is quite natural. However, under conditions of (50) even at arbitrary large  $\mu_\ell \rightarrow \infty$ , **PDP** is

$$D \approx \left(1 + \frac{1}{C_0}\right)^{\delta+1} \cdot F \approx \left(1 + \frac{\delta+1}{C_0}\right) \cdot F \leq \left(1 + \frac{1}{\delta+2}\right) \cdot F, \quad (53)$$

i.e. **not more than 1.5 times** exceeds **FAP**  $F$ .

This effect that seems to be paradoxical at **first sight** can be formally explained when analyzing **pdf** (40) transformation under conditions of (50) when **OSIR** is varied  $\mu = \mu_\ell$ . Fig. 2a shows a family of dependences  $g(x, C_1) = \sqrt{p_v(x, C_1)}$ ,<sup>2</sup>  $C_1 = C_0 \cdot (1 + \mu)$  for a set of values  $\mu = 0, 1, 9, 99$  ( $C_1 = C_0, 2 \cdot C_0, 10 \cdot C_0, 100 \cdot C_0$ ) given  $C_0 = 15$  and  $\delta = 2$ , when “small sample” conditions (50) are satisfied.

It is well seen that with the increase in  $\mu$  the **pdf**  $p_v(x, C_1)$  biases to the domain of **lesser**  $x$  values, and due to this, the **probability** to obtain values  $v \geq 1$  decreases. By virtue of (33a), (39b), (40), this means

<sup>2</sup> The use of the root of  $p_v(x, C_1)$  is inspired solely by a quest for image visualization. Otherwise it is inconveniently to simultaneously observe significantly “different in size” curves. With the same aim, a logarithmic scale on the  $x$ -axis is used that enables one to observe functions  $p_v(x, C_1)$  being significantly different in width for different values of  $C_1$ .

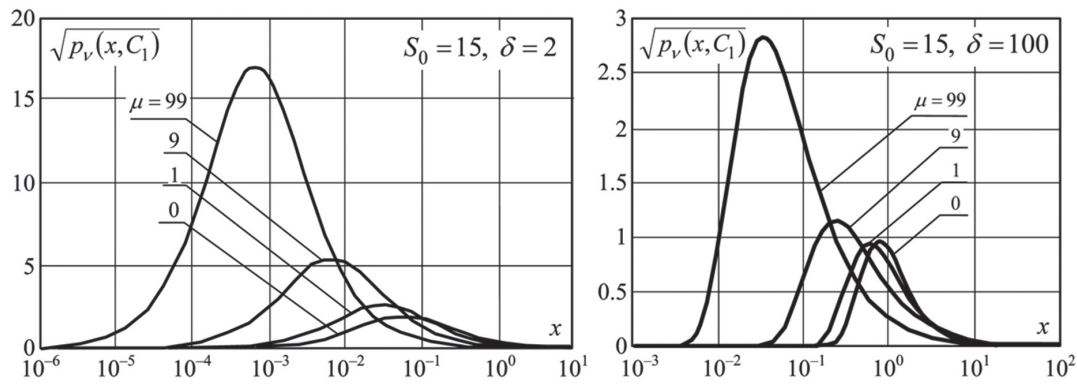


Fig. 2. (a) Pdf (40) transformation under conditions (50), when OSIR changes  $\mu = \mu_\ell$ .  
 (b) Pdf (40) transformation, when conditions (50) are not fulfilled and OSIR changes  $\mu = \mu_\ell$ .

that the probability to obtain the values of random SFs  $\hat{C}_3(\alpha)$  ( $\hat{S}_3(\alpha)$ ) being close to their true values  $C_3(\alpha)$  ( $S_3(\alpha)$ ) is the **less the more** these true values are. In this case, due to the pointed out “**bias to the left**”, the area under curve  $p_v(x, C_1)$  to the right of the point  $x = x_0/(1+\mu)$  defining  $D$  (see (42), (44)) remains practically the **same** as that under curve  $p_v(x, C_0)$  to the right of the point  $x = x_0$  defining  $F$ . This constitutes the fundamental difference between MCA and Capon’s MV method pdf (34) of whose normalized SF (33a) **does not depend** on the absolute true SF  $S(\alpha)$  level (the latter circumstance was noted as early as in [22, 23]).

As the effective sample size  $\delta$  grows (conditions (50) are violated), the “**bias to the left**” of densities  $p_v(x, C_1)$  (40) decreases with the increase in  $\mu$ , what is clearly seen in Fig. 2b given  $\delta = 100$ . Under these conditions, with the increase in  $\mu$ , PDP  $D$  also increases, however, rather slowly, and for each  $\delta$ , the **boundary** value  $\mu = \mu_b$  exists whose exceeding in practice already does **not increase** the value  $D = D_b$ . The  $\delta$  and  $\mu$  are related by the inequality

$$(\delta + 1) \cdot (\delta + 2) < C_1 = C_0 \cdot (1 + \mu). \quad (54)$$

When the inequality is satisfied, the first summand mainly contributes to sum (48), whereas contribution of the rest of summands can be neglected. In this case,

$$D = D_b \leq 1 - (C_0 \cdot x_0 / (1 + C_0 \cdot x_0))^{\delta + 1}. \quad (55)$$

In particular, under conditions of the example in Fig. 2b for  $F = 10^{-4}$  ( $x_0 = 100$ ), it follows that  $D_b \leq 0.06$  at any  $\mu \rightarrow \infty$ .

In this connection, requirements to the sample size for MCA can be **significantly higher** than those for the MV method. This is illustrated by the MCA detection characteristics shown in Fig. 3. Comparing them with the analogous curves in Fig. 1a for  $\delta = K - 1$ , it is easy to make sure that in the given examples, the performance provided by Capon’s method already for  $\delta = 0, 4, 19$ , is provided by MCA for  $\delta > 200, 400, 1000$  respectively.

D. Figs. 4a,b show the families of LP method pdfs like those in Figs. 2a, b, calculated by (39), (41). Figs. 5a, b display the empirical cumulative distri-

bution functions (cdfs) obtained with a mathematical model for distributions of SFs (1) normalized as (33a) of the BL and TN methods under conditions of Figs. 2 – 4. It is seen that the “**bias to the left**” effect with the increase in  $\mu$  is to this or that extent inherent in pdfs (cdfs) of normalized SFs of **all** the methods. The requirements to the effective sample size  $\delta$  for them, as well as for MCA, appear therefore to be **significantly higher** than those for the MV method. Reasons of the difference are discussed in Section VII.

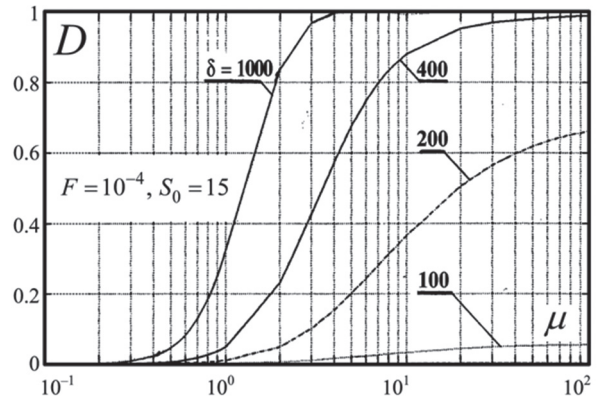


Fig. 3. Detection characteristics of MCA

E. The Capon’s MV method merits established compared with other methods (1) could become a decisive argument when choosing a direction finding method under conditions of the *a priori* uncertainty if a procedure of random SFs (1) comparison with the threshold  $v(\alpha)$  was practically realized at all the analysis points  $\alpha \in (\alpha_b, \alpha_e)$ . As follows from (43), this threshold is defined by a value of the true SF  $S_0 = S_0(\alpha)$  of corresponding method, i.e. by its value in the absence of source in the direction of analysis  $\alpha$ . The comparison with the threshold solely will provide the “record” (with minimum “payment”  $\varepsilon$  (46)) statistical detection performance of Capon’s method in the presence of source in the analyzed  $\alpha$ -direction.

But  $S_0$  is defined by CM  $\Phi_0$  (12) being *a priori unknown* and in reality this or that its estimate should be used instead of it. However unlike estimate (6) of CM  $\Phi$  (4), (9) **as a whole**, it is extremely difficult or even impossible to obtain estimate  $\hat{\Phi}_0$  of CM  $\Phi_0$  for all the  $\alpha \in (\alpha_b, \alpha_e)$  including  $\alpha = \beta_\ell$  ( $\ell \in 1, n$ )

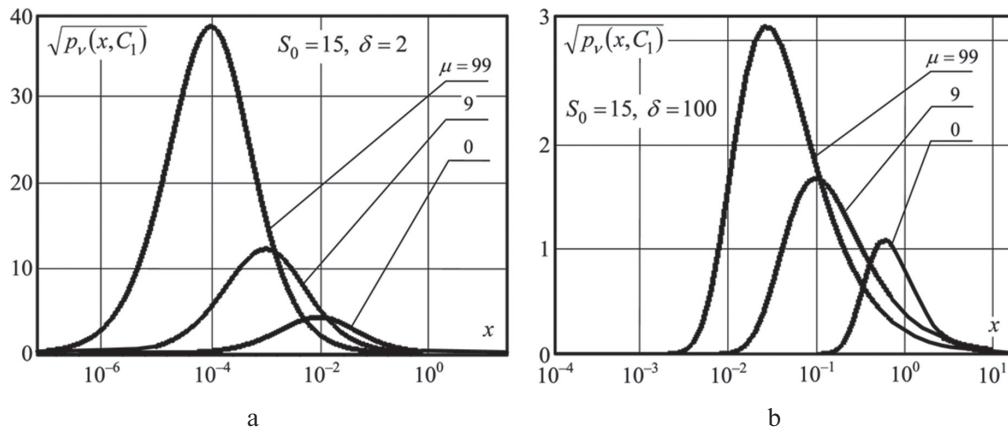


Fig. 4. (a) Pdfs of LP method under conditions (50), when OSIR changes  $\mu = \mu_\ell$ .  
 (b) Pdfs of LP method, when conditions (50) are not fulfilled and OSIR changes  $\mu = \mu_\ell$

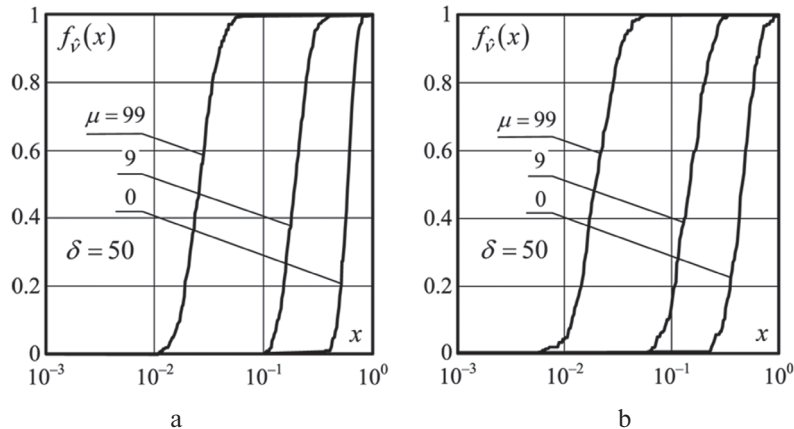


Fig. 5. (a) Empirical cdfs of normalized SFs of the BL method.  
 (b) Empirical cdfs of normalized SFs of the TN method

having available the **non-classified** at  $\alpha = \beta_\ell$  sample  $\mathbf{Y} = \{\mathbf{Y}_\ell\}_{\ell=1}^N$  only. Namely this can explain a wide spread in practice of other (**non-statistical**) resolution procedures and criteria, in particular the **Rayleigh** criterion not related to the **threshold** processing of SF  $\hat{S}(\alpha)$  at all the points  $\alpha$  of the analysis interval. The statistical analysis of methods (1) resolution by the (non-statistical) **Rayleigh** criterion is given below.

## VI. STATISTICAL ANALYSIS OF RESOLUTION BY THE RAYLEIGH CRITERION

**A.** Procedures for sources direction finding (the spatial spectral analysis) with methods (1) usually imply corresponding SFs  $\hat{S}(\alpha)$  formation at points  $\alpha$  of chosen sector  $(\alpha_b, \alpha_e)$  and a consequent search for their local **maxima**. The **number** of maxima is then identified with the **number**  $n$  of sources in this sector, whereas their **coordinates**  $\alpha_\ell$  and **values**  $\hat{S}(\alpha_\ell)$  ( $\ell \in 1, n$ ) are identified with the sources **directions** and relative **intensities** [1, 5, 6, 14, 25]. Resolution by the **Rayleigh** criterion is defined in a **test** scenario of two ( $n=2$ ) equipotent ( $q_1 = q_2 = q$ ) sources assumed to be resolved if the “**notch-depth**” between two maxima of  $\hat{S}(\alpha_\ell)$ ,  $\ell=1,2$ , characterized by the parameter

$$\hat{\gamma} = \frac{\hat{S}(\alpha_\ell)}{\hat{S}(\alpha_{mean})}, \quad \ell \in 1, 2, \quad \alpha_{mean} = \frac{\alpha_1 + \alpha_2}{2}, \quad (56)$$

exceeds the *a priori* chosen threshold  $\gamma_0$  (usually  $\gamma_0 = (1 \dots 3)$  dB) [1, 14, 25].

The goal of the following analysis is to compare resolutions of methods (1) on the basis of **ML** estimates (27), (6), (3) by criterion (56).

**B.** First, note that the (**forced**) proceeding from statistically optimal procedures and criteria to non-statistical ones inevitably entails **additional** energy consumption for resolution. For each of methods (1), the consumption is **different**. It is minimum under hypothetical conditions of **infinite** sample size  $N \rightarrow \infty$ , when the random SFs  $\hat{S}(\alpha)$  can be considered as coinciding with the **true** SFs  $S(\alpha)$  (by virtue of the asymptotic unbiasedness and consistency of **ML** estimates (27), (6)).

As is shown in [16-19], under these conditions, **MCA** is the “**best**” of methods (1), whereas the **MV** method is the “**worst**”. The asymptotic (for  $N \rightarrow \infty$ ) difference between them is quantitatively illustrated by Fig. 6 that shows **OSNR**  $q$  (23) values for each of two equipotent sources with angular distance  $\Delta$  (25) between them necessary for their resolution in **LUAA**.

Curves 1, 2, 3 here correspond to the **MV** method; curves 4, 5, 6 to **MCA**. In this case, curves 1, 4 are for  $\gamma=1$  and curves 2, 5 for  $\gamma=2$ . Curves 3, 6 specify the **boundary** values  $q = q_b$  at which the second derivatives  $d^2 S(\alpha)/d\alpha^2$  at point  $\alpha = \alpha_{mean}$  (56) of corresponding true SFs  $S(\alpha)$  are equal to zero [25]. For  $q \leq q_b$ ,



these SFs have a **single** maximum at point  $\alpha = \alpha_{mean}$ , so, by criterion (56), the sources are not **resolved**. They “start being resolved” when [16–19, 25]

$$\Delta \geq \begin{cases} \Delta_b \approx 1.17/\sqrt[4]{q_b} & \text{for the MV method,} \\ \Delta_b \approx 0.95/\sqrt[3]{q_b} & \text{for MCA.} \end{cases} \quad (57)$$

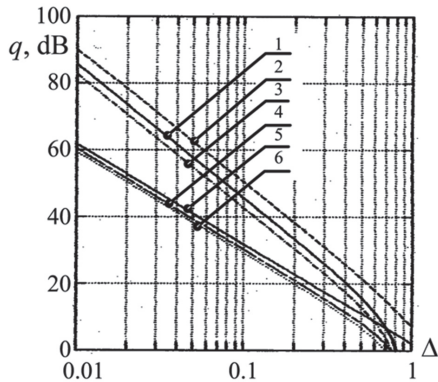


Fig. 6. Values of OSNR  $q$  (23) being necessary to resolve two equipotent sources with angular distance  $\Delta$

The  $q_b$  values for the rest of methods (1) are somewhat **higher** than those for **MCA**.

It is seen from a comparison of (57) with (26) that when using criterion (56), the less distance  $\Delta$  between sources, the higher additional energy consumption. In particular, for small  $\Delta \leq 0.1$ , it can constitute 10...20 dB and more.

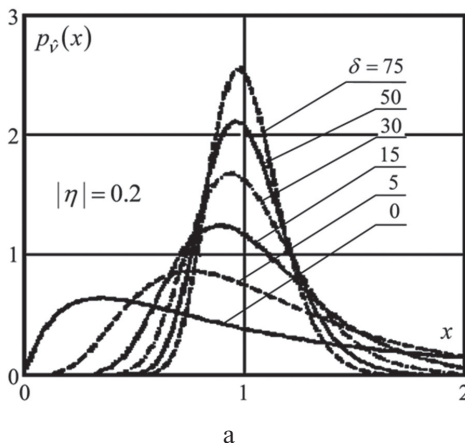
In a real **finite**  $N$  scenario, the consumption is even more due to resolution parameter  $\hat{\gamma}$  (56) randomness. It depends on statistical properties of  $\hat{\gamma}$ . The properties are **significantly different** for methods (1). This is demonstrated by the exact and experimental results to be discussed below.

**C.** For the **MV** method, the **pdf**  $p_{\hat{\gamma}}(x)$  of the normalized random parameter

$$\hat{\gamma} = \frac{\hat{\gamma}(\alpha_1, \alpha_2)}{\gamma(\alpha_1, \alpha_2)}, \quad \hat{\gamma}(\alpha_1, \alpha_2) = \frac{\hat{S}(\alpha_1)}{\hat{S}(\alpha_2)}, \quad \gamma(\alpha_1, \alpha_2) = \frac{S(\alpha_1)}{S(\alpha_2)} \quad (58)$$

given arbitrary  $\alpha_1 \neq \alpha_2$  and  $\delta \geq 0$  equals [15]

$$p_{\hat{\gamma}}(x) = \frac{\Gamma(2 \cdot \delta + 4)}{(\Gamma(\delta + 2))^2} \cdot \frac{(1 - |\eta|^2)^{\delta + 2} \cdot x^{\delta + 1} \cdot (1 + x)}{((1 + x)^2 - 4 \cdot |\eta|^2 \cdot x)^{\delta + 2.5}} \cdot (59)$$



Here

$$\eta = \mathbf{x}^*(\alpha_1) \cdot \Psi \cdot \mathbf{x}(\alpha_2) \cdot \sqrt{S_1(\alpha_1) \cdot S_1(\alpha_2)}, \quad (60)^{3*}$$

$$S_1(\alpha_i) = (\mathbf{x}^*(\alpha_i) \cdot \Psi \cdot \mathbf{x}(\alpha_i))^{-1}, \quad i = 1, 2$$

is the “generalized” spatial correlation coefficient of radiations from directions  $\alpha_1$  and  $\alpha_2$ , which coincides with (24) for  $\Phi = \Psi = \mathbf{I}_M$  and the vector  $\mathbf{x}(\alpha)$  in the form of (2).

At  $\delta \gg 1$ , for the mean  $\bar{\hat{\gamma}}$  and variance  $\sigma_{\hat{\gamma}}^2$  of parameter  $\hat{\gamma}$  (58), the following equalities are valid:

$$\bar{\hat{\gamma}} \approx 1 + \frac{1 - |\eta|^2}{\delta}, \quad \sigma_{\hat{\gamma}}^2 \approx \frac{2}{\delta} \cdot (1 - |\eta|^2). \quad (61)$$

An example of **pdfs** (59) for  $|\eta| = 0.2$  and different  $\delta$  values is given in Fig. 7a.

An **important property** of the **MV** method follows from analysis (59). It consists in that the random parameter  $\hat{\gamma}(\alpha_1, \alpha_2)$  given any effective sample sizes  $\delta \geq 0$  and values  $\alpha_1 \neq \alpha_2$  will be **not less** than its true value  $\gamma(\alpha_1, \alpha_2)$  (58) with the **fixed** probability  $P = 0.5$ . This statement is a consequence of the valid for (59) equality

$$p_{\hat{\gamma}}(x) = \frac{1}{x^2} \cdot p_{\hat{\gamma}}\left(\frac{1}{x}\right) \quad (62)$$

which means coincidence of **pdfs** (59) for positive random value  $\hat{\gamma} > 0$  (58) and its inverse  $\hat{\chi} = 1/\hat{\gamma}$ . This also means that, given any  $\alpha_1 \neq \alpha_2$ , the point  $x = x_0 = 1$  is the **pdf** (59) **median**, i.e.

$$\int_0^1 p_{\hat{\gamma}}(x) dx = \int_1^\infty p_{\hat{\gamma}}(x) dx = 1/2. \quad (63)$$

Indeed, by the normalization condition,

$$\int_0^\infty p_{\hat{\gamma}}(x) dx = \int_0^{x_0} p_{\hat{\gamma}}(x) dx + \int_{x_0}^\infty p_{\hat{\gamma}}(x) dx = 1.$$

But the first summand, by virtue of (62), is equal to

$$\int_0^{x_0} 1/x^2 \cdot p_{\hat{\gamma}}(1/x) dx = \int_{1/x_0}^\infty p_{\hat{\gamma}}(x) dx$$

and consequently,

3\*) A shape of density (59) keeps also being invariable when using ML estimates of persymmetric CMs in centrosymmetrical AA but in this case,  $\delta = N - (M + 1)/2$  [16 – 19].

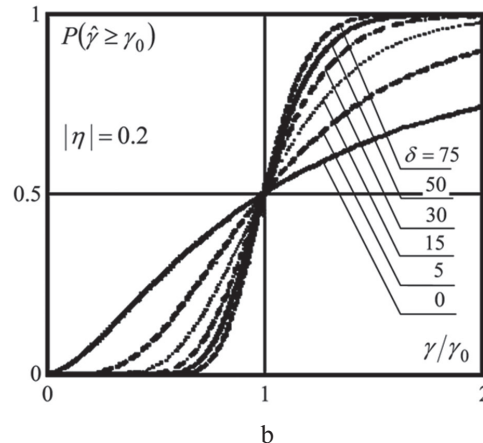


Fig. 7. (a) **pdfs** (59) at  $|\eta| = 0.2$  and different  $\delta$ . (b) The family of **cdfs** corresponding to **pdfs**  $p_{\hat{\gamma}}(x)$  (59)

$$\int_{1/x_0}^{\infty} p_{\hat{v}}(x) dx + \int_{x_0}^{\infty} p_{\hat{v}}(x) dx = 1,$$

whence equality (63) immediately follows. In combination with (58), it means that in the **MV** method,

$$P(\hat{v} \geq 1) = P(\hat{v} \geq \gamma_0 = \gamma) = 0.5 \text{ for any } \delta \geq 0. \quad (64)$$

These results were for the first time obtained in [15] and later corroborated in [48].

Equality (64) is a **mathematical formulation** of the described **MV** method property. It is illustrated by a family of the **cdfs** shown in Fig. 7b

$$f_v(\gamma/\gamma_0) = \int_0^{\gamma/\gamma_0} p_{\hat{v}}(x) dx = \int_{\gamma/\gamma_0}^{\infty} p_{\hat{v}}(x) dx = P(\hat{v} \geq \gamma_0) \quad (65)$$

accounted for the **pdfs**  $p_{\hat{v}}(x)$  (Fig. 7a).

By virtue of (62), these **cdfs** *de facto* describe the  $\Gamma = \gamma/\gamma_0$  dependence of the probability  $P(\hat{v} \geq \gamma_0)$  that the random parameter  $\hat{v} = \hat{v}(\alpha_1, \alpha_2)$  will be not less than the specified threshold  $\gamma_0$ .

As is seen from Fig. 7b, with the **increase** in the effective sample size  $\delta$ , the probability  $P(\hat{v} \geq \gamma_0)$  **grows** if  $\gamma > \gamma_0$ , keeps being **invariable** and equals 0.5 if  $\gamma = \gamma_0$ , and **decreases** if  $\gamma < \gamma_0$ . The formal reason of this is in transformation of **pdf**  $p_v(x)$  (59) (Fig. 7a), which, as  $\delta$  grows, “gathers” to the point  $x_0 = 1$ : its mean  $\bar{v}$  (61) tends to the median (the distribution “symmetrizes”), and the variance  $\sigma_{\hat{v}}^2$  decreases. This means that with the  $\delta$  growth, realizations  $\hat{v}$  concentrate in the more and more narrow vicinity of the true  $\gamma$  value. This increases (decreases) the probability that value  $\hat{v}$  exceeds the threshold  $\gamma_0$  being smaller (larger) than  $\gamma$ . However if  $\gamma_0 = \gamma$ , the probability  $P(\hat{v} \geq \gamma_0 = \gamma) = 0.5$  is constant for any  $\delta \geq 0$ .

Hence it follows that if a decision on resolution in a test (bisignal) scenario is made under condition that **at least one** of values at points  $\alpha_\ell$  of **SF**  $S(\alpha)$  maxima is  $\hat{v}_\ell = \hat{S}(\alpha_\ell) / \hat{S}_{mean}(\alpha) \geq \gamma_0$  ( $\ell = 1, 2$ ), then the resolution probability  $P_r$  by criterion (56), given  $\gamma = \gamma_0$ , will be equal to

$$P_r \leq P(\hat{v}_1 \geq \gamma_0) \cdot P(\hat{v}_2 < \gamma_0) +$$

$$+ P(\hat{v}_1 < \gamma_0) \cdot P(\hat{v}_2 \geq \gamma_0) + P(\hat{v}_1 \geq \gamma_0) \cdot P(\hat{v}_2 \geq \gamma_0) = \quad (66)$$

$$= P(\hat{v} \geq \gamma_0) \cdot (2 - P(\hat{v} \geq \gamma_0)) = 0.75,$$

where (64) and the evident equalities

$$P(\hat{v}_\ell < \gamma_0) = 1 - P(\hat{v}_\ell \geq \gamma_0), \quad P(\hat{v}_\ell \geq \gamma_0) = P(\hat{v} \geq \gamma_0),$$

$\ell = 1, 2$ , are taken into account.

An approximate nature of (66) is related to assumption of the events  $\hat{v}_1 \geq \gamma_0$  and  $\hat{v}_2 \geq \gamma_0$  independence, which is invalid in the general case (at small  $\Delta \ll 1$ ), as well as the non-unit probability of occurrence of two maxima in **SF**  $\hat{S}_1(\alpha)$  at any  $\delta \geq 0$  even given  $q > q_b$  (57).

It follows hence that curves 1, 2, 3 in Fig. 6 **not only** define the asymptotic (at  $\delta \rightarrow \infty$ ) **Capon's MV** method resolution, but also set requirements to the energy of two equipotent sources spaced at a distance  $\Delta < 1$  which for  $\gamma_0 = \gamma$  will provide their resolution by the **Rayleigh** criterion with the probability

$$0.5 \leq P_r < 0.75 \quad (67)$$

at any  $\delta \geq 0$ .

**D.** It should be expected that, by virtue of asymptotic unbiasedness and consistence of **ML** estimates (6), (3), analogous properties (64), (67) for  $\delta \rightarrow \infty$  will also be inherent in other methods (1) for which the exact **pdfs** of parameter  $\hat{v}$  (58) similar to (59) are not obtained yet. However, given finite  $\delta$ , attainment of “starting” probability  $P_r$  (67) on their basis is possible for the threshold  $\gamma_0 < \gamma$  only. Physical reasons of this are discussed in Section VII. Here, this statement is illustrated by the results of mathematical simulation.

Figs. 8a, b show families of the **cdfs**

$$f_v(x) = \int_0^x p_{\hat{v}}(y) dy \quad (68)$$

of parameter  $\hat{v}$  (58) of the **LP**, **MCA** and **MV** methods, given  $\delta = 0, 25, 50$ , for their **pdfs**  $p_{\hat{v}}(y)$  obtained experimentally.

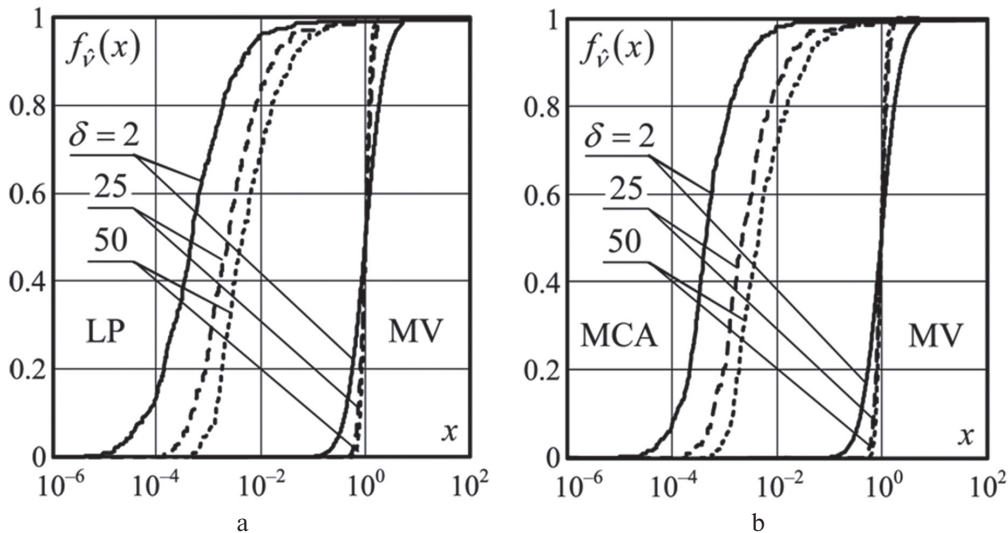


Fig. 8. Families of **cdfs** of parameter  $\hat{v}$  (58): (a) for the **LP** and **MV** methods; (b) for the **MCA** and **MV** methods

The scenario is simulated for two ( $n = 2$ ) equi-potent sources with the relative distance  $\Delta = 0.1$  between them for  $q_1 = q_2 = q = 50.5$  (dB). Under these conditions, the **true**  $\gamma$  values are equal to 2 (3 dB) for the **MV** method and  $\gamma > 10^3$  (30 dB) for the **LP** and **MCA** methods.

It is clearly seen that for the **MV** method the parameter  $\hat{\nu}$  (58) median is equal to  $x = x_0 = 1$  regardless of  $\delta$ , what fully conforms to the above theory. At the same time, medians of distribution functions (67) of the **LP** and **MCA** methods are located significantly more to the left of the point  $x_0 = 1$  ( $x_0 \approx 5 \cdot 10^{-4}$  for  $\delta = 2$  and  $x_0 \approx 5 \cdot 10^{-3}$  for  $\delta = 50$ ). Therefore, probability  $P_r$  (67) of resolution with these methods is provided when choosing the threshold  $\gamma_0 = x_0 \cdot \gamma \ll \gamma$  even for  $\delta \geq 50$ . The **BL** and **TN** methods also yield the results **close to aforementioned**.

Hence, it follows that **asymptotic** ( $\delta \rightarrow \infty$ ) energy **gains** of methods (1) compared to the **MV** methods, which ensue from Fig. 6, by no means **guarantee** that their resolution probability by **Rayleigh** criterion (56) under **realistic** conditions of finite  $\delta$  will be higher than that obtained with the **MV** method.

The results of experimental comparison of methods (1) under these conditions are given in Fig. 9 in the form of dependences  $P_r(\delta)$  given  $\Delta = 0.8$ ,  $q = 10$  dB and the resolution threshold  $\gamma_0 = 1.5$  ( $\approx 1.8$  dB) that coincides with the  $\gamma$  value of the **MV** method. The  $\gamma$  values of the rest of methods are given in brackets under their abbreviations.

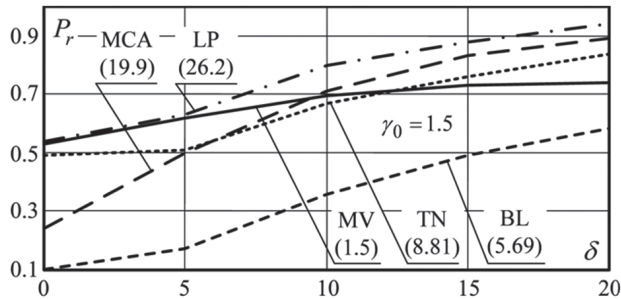


Fig. 9. The results of experimental comparison of methods (1)

As is seen from the figures, in the **MV** method, as  $\delta$  grows, the resolution probability monotonically increases from  $P_r \approx 0.5$  to  $P_r \approx 0.75$ , that is **namely so** as it has to theoretically vary at  $\gamma_0 = \gamma$ . At the same time the rest of methods at small  $\delta \leq 10$  either insignificantly exceed (**LP**) or are even **worse** in efficiency than the **MV** method, although the values corresponding to them are  $\gamma > \gamma_0$ .

Thus for finite  $\delta$ , all the methods (1) have **essentially worse** statistical properties than **Capon's MV** method. Their real resolution by both statistical (Section V) and non-statistical (Section VI) criteria under these conditions is therefore significantly worse than the asymptotic one (at  $\delta \rightarrow \infty$ ).

Reasons of the difference and ways following from them for enhancement of methods (1) "**robustness**" are discussed below.

## VII. REASONS OF DIFFERENCE IN STATISTICAL PROPERTIES AND WAYS OF THEIR IMPROVEMENT

A. The above established "**special**" place of **Capon's MV** method among methods (1) under conditions of finite effective sample size  $\delta \geq 0$  can be explained using **interrelation** between their **SFs** as well as the specific **SF** property of the **MV** method itself. These interrelation and property are commonly known (see, e.g., [1 – 6, 14, 27, 32 etc.]) and, as a rule, used for explanation of the difference between corresponding methods under hypothetic conditions of **exact CM**  $\Phi$  (4), (9).

Let us begin from this situation, considering the "**true**" **SFs**  $S(\alpha)$  obtained by replacing matrix  $\Psi$  (3) in random **SFs**  $\hat{S}(\alpha)$  by "**true**" matrix  $\Psi$  (11).<sup>4\*</sup>

B. Introduce the  $m$  th ( $m \in 1, M$ ) order **SF** of the **MV** method

$$S_1(\alpha, m) = \left( \mathbf{x}_m^*(\alpha) \cdot \Psi_m \cdot \mathbf{x}_m(\alpha) \right)^{-1}, \quad (69)$$

$$\mathbf{x}_m(\alpha) = \{x_i(\alpha)\}_{i=1}^m, \quad \Psi_m = \Phi_m^{-1}, \quad \Phi_m = \{\varphi_{ij}\}_{i,j=1}^m.$$

The **SF**  $S_1(\alpha, M-1)$  is related to the **SF**  $S_1(\alpha) = S_1(\alpha, M)$  by the equality [1, 3, 17, 27, 32]

$$S_1^{-1}(\alpha, M) = S_1^{-1}(\alpha, M-1) + S_{ME}^{-1}(\alpha),$$

$$S_{ME}(\alpha) = \frac{\omega_{MM}}{|\mathbf{e}_M^*(\alpha) \cdot \Psi \cdot \mathbf{x}_M(\alpha)|^2} = S_2(\alpha), \quad m = M, \quad (70)$$

where  $S_{ME}(\alpha)$  is **SF** of **Burg's** "maximum entropy" (**ME**) method [24, 32], which given  $m = M$  coincides with the **SF**  $S_2(\alpha)$  of **LP** method (1).

Hence and from a comparison of the first three **SFs** in (1), it follows that

$$S_{ME}(\alpha) = S_3(\alpha) \cdot S_1(\alpha, M) = C_3(\alpha) \cdot S_1(\alpha, M-1) = S_2(\alpha), \quad m = M, \quad (71a)$$

$$S_3(\alpha) = \frac{S_1(\alpha, M-1)}{S_1(\alpha, M-1) - S_1(\alpha, M)}, \quad (71b)$$

$$C_3(\alpha) = \frac{S_1(\alpha, M)}{S_1(\alpha, M-1) - S_1(\alpha, M)} = S_3(\alpha) - 1.$$

Consider functions  $S_3(\alpha)$  or  $C_3(\alpha)$  more in detail. Let us begin from their values at points  $\alpha = \beta_\ell$  ( $\ell \in 1, n$ ) of **sources location** when the steering vector  $\mathbf{x}(\alpha) = \mathbf{G} \cdot \mathbf{e}_\ell$  coincides with the  $\ell$  th column of matrix  $\mathbf{G}$  (9). As follows from (69), (11), in this case,

$$S_1^{-1}(\beta_\ell, M) = \mathbf{e}_\ell^* \cdot \mathbf{Q} \cdot (\mathbf{I}_n - \mathbf{T}) \cdot \mathbf{e}_\ell,$$

$$\mathbf{T} = \left( \mathbf{I}_n + (\mathbf{h} \cdot \mathbf{Q})^{-1} \right)^{-1}, \quad \mathbf{Q} = \mathbf{G}^* \cdot \mathbf{G}. \quad (72)$$

<sup>4\*</sup> Note that here we for the first time use in the theoretical treatment the specific peculiarities of structures of **CM**  $\Phi$  (9) and  $\Psi$  (11) (which are used above for quantitative assessment only). All the analytical results of Sections IV – VI are therefore true not only for these **CMs**, but also for **arbitrary CMs** of Gaussian processes (e.g., corresponding to **correlated radiations**, **spatially distributed radiation sources** (reflections), etc.)

Let maximum eigenvalue  $\lambda_{\max}(\mathbf{W})$  of matrix  $\mathbf{W} = (\mathbf{h} \cdot \mathbf{Q})^{-1}$  satisfy the condition

$$\lambda_{\max}(\mathbf{W}) = \lambda_{\min}^{-1}(\mathbf{W}^{-1}) = \lambda_{\min}^{-1}(\mathbf{h} \cdot \mathbf{Q}) \ll 1, \quad (73)$$

whereat for matrix  $\mathbf{T}$  the following approximate equality is valid:

$$\mathbf{T} \approx \mathbf{I}_n - (\mathbf{h} \cdot \mathbf{Q})^{-1}.$$

Then  $S_1^{-1}(\beta_\ell, M) \approx \mathbf{e}_\ell^* \cdot \mathbf{h}^{-1} \cdot \mathbf{e}_\ell$ , so in the considered case of independent radiations (diagonal matrix  $\mathbf{h}$  (9))

$$S_1(\beta_\ell, M) \approx h_\ell, \quad \ell \in 1, n. \quad (74)$$

Equality (74) had been repeatedly mentioned in the literature, but its fulfilment had been linked either to the presence of distinct maxima in SF  $S_1(\alpha)$  in the vicinity of points  $\beta_\ell$  ( $\ell \in 1, n$ ) or to even more rigorous requirement  $h_\ell \rightarrow \infty$  [6]. It is essential, however, that it is valid in the “preasymptotic” domain as well, i.e. at smaller OSNR values  $q_\ell$  than it is required for the occurrence of these maxima in the SF  $S_1(\alpha)$ .

Let us show this on the example of the  $M$ -element LUAA in the ( $n=2, \Delta \leq 1, \mathbf{h} = h \cdot \mathbf{I}_2, q_1 = q_2 = q = M \cdot h$ ) test scenario. In this case,  $\lambda_{\min}(\mathbf{h} \cdot \mathbf{Q}) = q \cdot (1 - \rho)$ , so condition (73) is equivalent to the condition  $q \gg (1 - \rho)^{-1}$  which can be considered as satisfied already with

$$q = M \cdot h = q_0 \geq 10 \cdot (1 - \rho)^{-1}, \quad (75)$$

$$\rho = \frac{\sin(\pi \cdot \Delta)}{\pi \cdot \Delta} = \sum_{i=0}^{\infty} \frac{(-1)^i \cdot (\pi \cdot \Delta)^{2i}}{(2 \cdot i + 1)!}.$$

The less  $\Delta$ , the larger  $q_0$  (75) values but given small  $\Delta < 0.5$ , when for  $\rho$  the presentations

$$\rho \approx 1 - \pi^2 \cdot \Delta^2 / 6 \approx 1 - 1.5 \cdot \Delta^2, \quad 1 - \rho \approx 1.5 \cdot \Delta^2 \quad (76)$$

are valid, requirement (73), which leads to equality (74), for  $q_0 \geq 7/\Delta^2$  is also satisfied. This value of  $q_0$  is approximately  $(2 \cdot \Delta)^{-2}$  times less than  $q_b$  (57) of the MV method.

Growth of OSNR  $q$  to higher values than “boundary” value  $q_0$  (15) practically does not change  $S(\beta_\ell)$ ,  $\ell \in 1, n$  (74), so for any

$$q > q_0, \quad q_0 < q_b,$$

the normalized SF  $S_1(\alpha, M)/h$  at points  $\alpha = \beta_\ell$  of sources location equals

$$S_n(\beta_\ell) = S_1(\beta_\ell, M)/h \approx 1. \quad (77)$$

Fig. 10a shows a family of normalized SFs (77) for the test scenario in LUAA given  $\Delta = 0.1$ , when  $q_0 \approx 700$  (28 dB). The  $q \in [20, 56]$  dB serves as the family parameter; sources location is shown by arrows.

It is well seen that

$$S_n(\beta_\ell) > 1 \text{ for } q < q_0, \quad q_0 < q_b, \quad (78)$$

but with increase in  $q \geq q_0$ , values  $S_n(\beta_\ell)$  approach from top to unit (“stick together”) at points of true location of sources [17] even before the occurrence of “distinct” maxima in the  $S_n(\alpha)$ .

Now let us pay attention that condition (73) and equalities (74), (77), (78) ensuing from it are formulated for OSNR  $q$ , but not for its multipliers in (75) apart. Even for the fixed SNR  $h_\ell = h$  at the points  $\alpha = \beta_\ell$ , SFs of all the orders  $m \leq M$  of MV methods, whereat equalities  $q_m = m \cdot h \geq q_0$  (75) are satisfied, are therefore close to each other (“stick together”).

Hence, it follows that when  $M \gg 1$  and (73), (75) are valid,

$$S_1(\alpha, M - 1) - S_1(\alpha, M) \geq 0, \quad \alpha = \beta_\ell, \ell \in 1, n, q \geq q_0 \quad (79)$$

and the more  $q \geq q_0$ , the closer this positive difference to null.

The small difference in denominators of the MCA SFs  $S_3(\alpha)$  or  $C_3(\alpha)$  (71b) under conditions (79) entails the distinct maxima in these SFs (resolution by criterion (56)) with less OSNR  $q$  values than those required for the MV method SFs  $S_1(\alpha)$  being basic for the MCA SFs. This reveals itself when comparing families of SF  $C_3(\alpha)$  (71b) shown in Fig. 10b with families of SF  $S_1(\alpha)$  shown in Fig. 10a, as well as curves 4, 5, 6 with curves 2, 3 in Fig. 6.

By virtue of equalities (71a), the ME method given exact CM has the performance being close to that of MCA by criterion (56) and significantly exceeding that of the basic MV method. Besides, the established in [27] relations between SFs of the ME (LP) and TN methods show that the latter, being insignificantly worse than the ME method, under

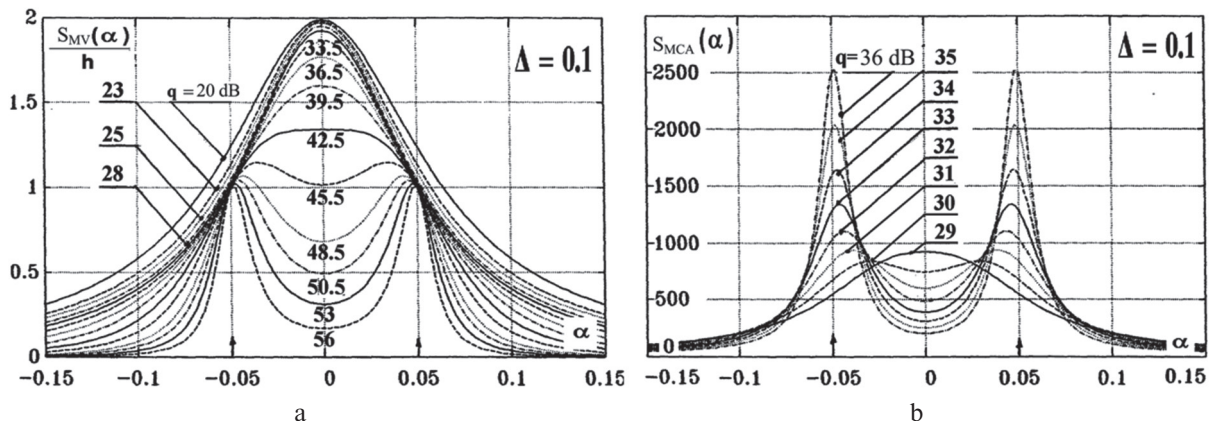


Fig. 10. (a) Family of normalized SFs (77). (b) Family of SF  $C_3(\alpha)$  (71b)

these conditions can also significantly exceed the **MV** method. The same concerns the **BL** method whose **SF**  $S_4(\alpha)$  in the “liaison”

$$S_5(\alpha) = S_4(\alpha) \cdot S_1(\alpha) \quad (80)$$

between **SFs**  $S_5(\alpha)$  and  $S_1(\alpha)$  of the **TN** and **MV** methods plays the same role as **SFs**  $S_3(\alpha)$  or  $C_3(\alpha)$  of **MCA** in “liaison” (71a).

Thus, in each of methods (1), there is used to this or that extent property (74), (77) of “**sticking together**” of **SFs**  $S_1(\alpha)$  of the **MV** method of orders  $M$  and  $M-1$  at points  $\alpha = \beta_\ell$ ,  $\ell \in 1, n$  of sources location under conditions (73), (75). It is not used in the **MV** method itself only, and namely for this reason in the hypothetic situation of exactly known **CM**  $\Phi$  (4), (9) it has the “worse” resolution performance by criterion (56) than that of the rest of the methods (see Section VI-B, Fig. 6).

**C.** However, in the realistic situation of the estimation **CMs**  $\hat{\Phi}$  (6), (27) and the finite size  $\delta \geq 0$  samples, fine “**sticking together**” effects (79) can be **breakdown** by random errors of **CM** estimation. These “destructions” can be of two kinds.

**First**, the random difference

$$\hat{S}_1(\alpha, M-1) - \hat{S}_1(\alpha, M) \geq 0, \quad (81)$$

which keeps being non-negative, with the non-zero probability can be **less** than true one (79) in the **absence** of sources in the direction of analysis  $\alpha$ . Namely this makes heavier **tails** in distribution (40) and requires to significantly increase the threshold constant  $x_0$  to fix **FAP**  $F$  for the **MCA** method as well as for the **LP**, **BL**, **TN** ones (Section V-C, D).

**Second**, random difference (81), which is defined by the **CM** estimation **errors**, can be **larger** than true one (79) and **independent** of it at an arbitrary level of radiation in the direction of analysis  $\alpha = \beta_\ell$ , ( $\ell \in 1, n$ ). This explains the “**bias to the left**” of the aforementioned methods **pdfs** and **cdfs** (Sections V, VI), as well as the paradoxical, at first sight, **constancy** of the **PDP** level  $D$  in **MCA** at arbitrarily large values of  $\infty$ . The smaller effective sample size  $\delta \geq 0$ , the smaller  $D$  (Section V-C).

Namely for this reason **Capon's** **MV** method, wherein the easily destructible “**sticking together**” effects are **not used**, appear to be the most “**robust**” under these conditions.

The analytical and experimental results of Sections V, VI yield the quantitative characteristics of the described consequences of the conditions (79), (74) “**breakdown**” subject to the effective sample size  $\delta \geq 0$  for each of methods (1). Allowance for them and the understanding of the described physical mechanism enable us to propose simple modifications of **SFs** (1) with significantly better statistical characteristics.

## VIII. KINDS OF “SUPERRESOLVING” DOA ESTIMATORS

**A.** At the beginning, note that values of **SFs**  $\hat{S}(\alpha)$  (1) of the **MV**, **LP** methods and **MCA** at an arbitrary

point  $\alpha \in [\alpha_b, \alpha_e]$  of analysis can be obtained combining squared modules of elements of the vector

$$\begin{aligned} \mathbf{p} &= \mathbf{p}(\alpha) = \{p_m(\alpha)\}_{m=1}^M = \hat{\mathbf{H}} \cdot \mathbf{x}, \\ \mathbf{x} &= \mathbf{x}(\alpha), \quad \alpha \in [\alpha_b, \alpha_e]. \end{aligned} \quad (82)$$

Here  $\mathbf{x}(\alpha)$  is the steering vector similar to (2);  $\hat{\mathbf{H}} = \{h_{i\ell}\}_{i,\ell=1}^M$  the  $M \times M$  lower ( $h_{i\ell} = 0$  for  $\ell > i$ ) triangular matrix that is **Cholesky** multiplier of  $\hat{\Psi}$  (3) presented as

$$\hat{\Psi} = \hat{\mathbf{H}}^* \cdot \hat{\mathbf{H}} \quad (83)$$

which under conditions (5) exists for any  $\delta = N - M \geq 0$ .

It is easy to make sure that in these designations

$$\begin{aligned} \hat{S}_1(\alpha) &= (\mathbf{p}^* \cdot \mathbf{p})^{-1} = \left( \sum_{m=1}^M |p_m|^2 \right)^{-1} = \\ &= (\mathbf{p}_{-M}^* \cdot \mathbf{p}_{-M} + |p_M|^2)^{-1}, \quad \mathbf{p}_{-M} = \{p_m\}_{m=1}^{M-1}, \end{aligned} \quad (84a)$$

$$\begin{aligned} \hat{S}_{ME}(\alpha) &= |p_M|^{-2} = (\mathbf{p}^* \cdot \mathbf{p} - \mathbf{p}_{-M}^* \cdot \mathbf{p}_{-M})^{-1} = \\ &= \hat{S}_2(\alpha), \quad m = M, \end{aligned} \quad (84b)$$

$$\hat{S}_3(\alpha, M) = \frac{\mathbf{p}^* \cdot \mathbf{p}}{|p_M|^2} = \hat{C}_3(\alpha) + 1, \quad (84c)$$

$$\hat{C}_3(\alpha) = \frac{\mathbf{p}_{-M}^* \cdot \mathbf{p}_{-M}}{|p_M|^2}, \quad m = M.$$

When deriving (84b), it is taken into account that by virtue of (83),

$$\hat{\omega}_{MM} = \hat{h}_{MM}^2, \quad \mathbf{e}_M^* \cdot \hat{\mathbf{H}}^* = h_{MM} \cdot \mathbf{e}_M^*.$$

**B.** As is seen from (84b), **SF**  $\hat{S}_{ME}(\alpha) = \hat{S}_{ME}(\alpha, M)$  (70) is defined by squared module of a **single** (last) element  $p_M$  of the vector  $\mathbf{p} = \{p_m\}_{m=1}^M$  (82), whereas the **SF**  $\hat{S}_1(\alpha)$  is defined by squared modules of **all** the vector elements. The squared  $m$ th element module as a function of  $\alpha$  has a meaning of radiation pattern (**RP**) of the  $m-1$  order spatial linear prediction filter with minimum RMS in the  $m$ -element **AA** with the decreased (in the case of **LUAA**,  $M/m$  times) aperture size. The less  $m$ , the “smoother” these **RPs** as functions of  $\alpha$  (in particular, the **SF**  $|p_1|^{-2}$  do not depend on  $\alpha$  at all). Namely this full accumulation of the **all** the orders  $m \in 1, M$  **SFs**  $\hat{S}_{ME}(\alpha, m)$  with different degrees of smoothing explains both asymptotically (at  $N \rightarrow \infty$ ) minimum **Capon's** method resolution compared to other methods (1) by **Rayleigh** criterion (Section VI-B) and its maximum “**robustness**” under conditions of small effective sample size  $\delta = N - M \geq 0$  (Sections V-B, VI-C, VII). And vice versa, namely the full **absence** of accumulation of the smoother  $m < M$  order **SFs**  $\hat{S}_{ME}(\alpha, m)$  causes significantly higher resolution, by the **Rayleigh** criterion, of the **ME** method given  $N \rightarrow \infty$  due to the “**sticking together**” effect, as well as its minimum “robustness” in conditions of small  $\delta \geq 0$  when the effect **breakdowns** (Sections V-D, VI-D, VII).

In this connection, in real scenarios of finite-size sample, more useful can be “intermediate” SFs  $\hat{S}_{int}(\alpha)$  looking like [33]

$$\hat{S}_{int}(\alpha) = (\mathbf{p}^* \cdot \mathbf{p} - \mathbf{p}_{\chi \cdot M}^* \cdot \mathbf{p}_{\chi \cdot M})^{-1} = (\mathbf{p}_{int}^* \cdot \mathbf{p}_{int})^{-1}, \quad (85a)$$

$$\mathbf{p}_{\chi \cdot M} = \{p_m\}_{m=1}^{\chi \cdot M}, \quad \mathbf{p}_{int} = \{p_m\}_{m=1+\chi \cdot M}^M.$$

They are formed by the “intermediate” number

$$n_{int} = (1 - \chi) \cdot M, \quad \chi \in 0, (M-1)/M \quad (85b)$$

of last components of the vector  $\mathbf{p}$  or, what is equivalent, its first  $\chi \cdot M$  components are **excluded** from them. In the boundary cases  $\chi = 0$  and  $\chi = (M-1)/M$ ,

$$\hat{S}_{int}(\alpha) = \begin{cases} \hat{S}_1(\alpha), & \chi = 0, & n_{int} = M, \\ \hat{S}_E(\alpha), & \chi = (M-1)/M, & n_{int} = 1. \end{cases} \quad (85c)$$

“Intermediate” variants of MCA SF (84c), for whose designation we use ( $\sim$ ) instead of ( $\hat{\cdot}$ ), take the form:

$$\tilde{S}_3(\alpha) = \mathbf{p}^* \cdot \mathbf{p} / \mathbf{p}_{int}^* \cdot \mathbf{p}_{int} = \tilde{C}_3(\alpha) + 1, \quad (85d)$$

$$\tilde{C}_3(\alpha) = \mathbf{p}_{\chi \cdot M}^* \cdot \mathbf{p}_{\chi \cdot M} / \mathbf{p}_{int}^* \cdot \mathbf{p}_{int}.$$

**C.** The proceeding from SFs (84) to “intermediate” SFs (85) is accompanied by two “fighting” effects. On the one hand, their asymptotic ( $N \rightarrow \infty$ ) resolution increases to be the closer to the ME method (84b) resolution, the closer value  $\chi$  is to the upper bound  $\chi = (M-1)/M$ . On the other hand, their “robustness” decreases in conditions of small effective size  $\delta = N - M \geq 0$ , when the “sticking together” effect **breakdowns** (Section VII). Therefore, an expediency of intermediate SFs (85) depends on which of effects stronger reveals itself.

A comparative theoretical analysis of the effects impact [33] has shown that there exists a rather wide parameter domain  $0 < \chi < (M-1)/M$  wherein “intermediate methods (85a), (85d) under conditions of small size sample appear to be significantly more efficient than their “boundary” analogues (84), (85c) with  $\chi = 0$  or  $\chi = (M-1)/M$ .

As an example, for the  $M = 16$ -element LUAA given different values of the parameter

$\chi \in 0, (M-1)/M \approx 0.94$ , Fig. 11 shows modeling dependences of the resolution probability  $P_r(\delta)$  given the resolution threshold  $\gamma_0 = \gamma_{MV} = 2$  dB (Section VI-C, D) for SFs  $\hat{S}_{int}(\alpha)$  (85a) (Fig. 11a) and  $\tilde{C}_3(\alpha)$  (85d) (Fig. 11b).

It can be seen that, already with small effective sample sizes  $\delta = N - M \geq 0$ , the “intermediate” SFs

$\hat{S}_{int}(\alpha)$  provide resolution by the **Rayleigh** criterion with such a probability that is either provided by their “boundary” kinds ( $\hat{S}_E(\alpha)$ ) given significantly larger sample size  $\delta \gg 1$  ( $\hat{S}_E(\alpha)$ ) or not provided at all ( $\hat{S}_V(\alpha)$ ). It is also seen that the “intermediate” SFs  $\tilde{C}_3(\alpha)$  are more efficient than the “intermediate” SFs  $\hat{S}_{int}(\alpha)$  given small values  $\delta \geq 0$  and not worse than they at any  $\delta \gg 1$ .

**D.** Of a great many of possible in principle filters with MIC  $\hat{\mathbf{H}}$ , the most interesting are adaptive lattice filters (ALF) [37 – 40]. Having the input steering vector  $\mathbf{x}(\alpha)$ , simply combining squared modules of output signals of the tuned ALFs, it is possible to realize not only considered SFs (1), (85) but a diversity of their kinds with practically useful properties. In typical cases of  $M \gg 1$  their aggregate forms a rather capacious “bank” of noneigenstructure (NES) methods of DoA estimation. On its basis, the proposed by **A. Gershman** idea [12, 43 – 46] of combined direction finding with an aggregate of “superresolving” DoA estimators can be easily realized. He has shown that in this case, using a respective strategy, it is possible to obtain the higher **efficiency** of DoA estimation, and besides to reduce requirements to the sample size compared with each of the “bank” methods apart.

**E.** Specificity of the “banks” proposed in [12, 43 – 46] is in insertion in them of DoA estimators realizing “eigenstructure (ES)” methods of MUSIC type [1 – 4, 7]. Their high potential efficiency is based on allowing for the *a priori* information that a signal constituent rank of the correlation matrix of  $M > 1$  spatial receive channels output signals is equal to the number  $n < M$  of external independent sources. However, such an equality corresponds to an idealized scenario

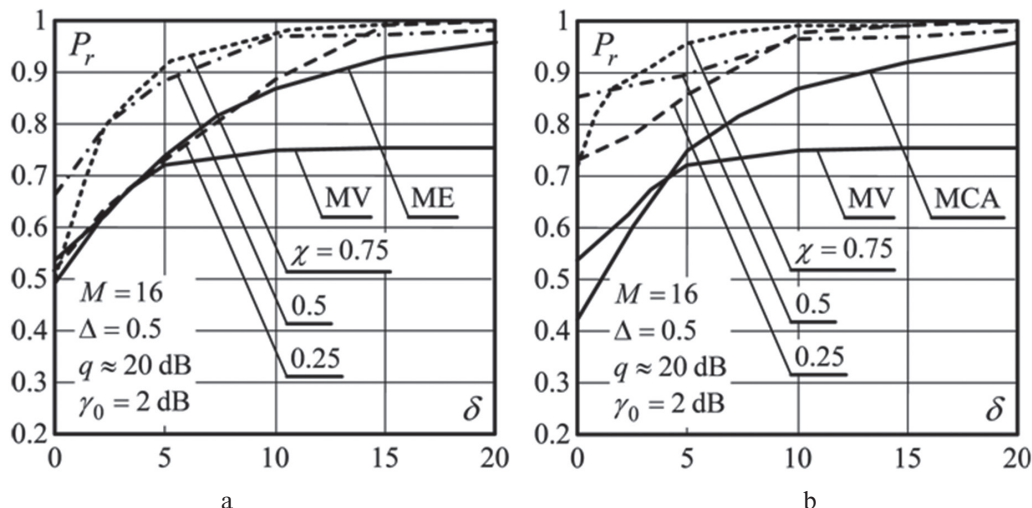


Fig. 11. The results of experimental comparison of methods (85)

of exact matching of a **CM** model used as the basis for the **ES** methods synthesis and the real **CM** that can differ from the model for a number of reasons.

One of reasons of this is practically inevitable non-identity of frequency (pulse) characteristics of spatial receive channels. As a special testing has shown [41, 42], this effect essentially differently impacts on efficiencies of “**ES-bank**” and **ALF**-based “**NES-bank**”. The “**ES-bank**” can become practically unserviceable at such a level of non-identity whereat the “**NES-bank**” efficiency decreases insignificantly. Therefore, it is expedient to use namely the **ALF**-based bank when realizing in practice fruitful **Gershman’s idea** of combined **DoA** estimation for point sources radiation.

## CONCLUSIONS

The paper is devoted to the investigations of a number of known “superresolving” methods resolution for **DoA** estimation of point sources noise radiation in an  $M$ -element antenna array (**AA**) given a finite-size sample, and to substantiation on this basis of their new variants with heightened efficiencies under these conditions.

1. From the **Shirman’s** statistical theory positions, potentialities of **resolution-detection** are defined for Gaussian noise signals of point sources against the background of Gaussian self-noise of  $M$  receive channels. They are provided under hypothetic conditions of full *a priori* definiteness and optimal processing of available  $K$ -variate sample of  $M$ -variate vectors of complex amplitudes of the additive signal and noise mixture at the receive channel outputs. **Shirman’s** classic results related to the case of  $K=1$ , are generalized to the case of arbitrary  $K$ . It is shown that in the test  $n=2$  equipotent sources with **SNR**  $q$  scenario a minimum angular distance between sources under resolution for  $D=0.5$  and  $F=10^{-6}$  is inversely proportional to  $\sqrt{q}$  if  $K=1$  and to  $q$  if  $K>30$ . In real conditions of the *a priori* uncertainty, **additional** signal energy consumption is needed for resolution (Section III).

2. A degree of proximity to the established potentialities is estimated for efficiencies of five known “noneigenstructure” (**NES**) methods of spectral analysis (**SA**). Their spectral functions (**SF**) are defined by a matrix being inverse to the maximum likelihood (**ML**) estimate of the correlation matrix (**CM**) of the input mixture under analysis. It is assumed that it is formed by a  $N \geq M$ -size sample and has well-known **Wishart’s** complex distribution. The sample size  $N \geq M$  dependence of these methods resolution-detection by the statistical criterion is estimated. It is shown that “payment”  $\varepsilon$  for the *a priori* lack of knowledge of **CM** is minimum in **Capon’s** method. Given already  $N = K + \varepsilon$  with  $\varepsilon = M - 1$ , this method provides the same statistical characteristics of the threshold detection as those provided by the optimal threshold processing of the  $K$ -variate sample in the absence of the *a priori* uncertainty (given exactly known **CM** by hypotheses of the presence and absence

of “useful” signal). In the rest of the methods, “payment” for a lack of knowledge is significantly higher, what is explained by the revealed effect of these **SF**s distribution densities “**bias to the left**” with growth of radiation intensity (Sections IV, V).

3. It is difficult to realize in real conditions of the *a priori* uncertainty the established **Capon** method advantages, since the information necessary for setting a corresponding detection threshold is usually absent. In this connection, there is analyzed resolution of the methods under consideration by the widely used **non-statistical Rayleigh** criterion for two equipotent harmonics resolution.

It is shown that in a hypothetic asymptotic scenario ( $N \rightarrow \infty$ ), the best of the considered methods by this criterion is the Modified **Capon** Algorithm (**MCA**). When using it, a distance between resolvable harmonics is inversely proportional to the cubic root of their relative intensity  $q$ . The worst of them is the **Capon** method (the distance is inversely proportional to the fourth root of  $q$ ). However, under real conditions of finite  $N \geq M$  they can “switch places”. This is related to the specificity of distribution density of ratio of **Capon** method **SF** values at two points, which consists in that this (random) ratio given any sample size  $N \geq M$  with the fixed probability  $P=0.5$  is not less than its true value in the absence of the *a priori* uncertainty.

In order to provide such a probability with other methods, much larger-size samples are needed. In real situations of finite size samples, the **Capon** method resolution can therefore be not less and even higher than that of the rest of methods (Section VI).

4. Physical reasons of better statistical properties of the **Capon** method **SF** are explained. It is shown that the rest of the methods to this or that extent use the “**sticking together**” effect of exact different order **SF**s of the **Capon** method at points of true sources location even before distinct maxima occur in these **SF**s in the sources directions. This property is not used in the **Capon** method itself only. And namely for this reason under hypothetic asymptotic conditions ( $N \rightarrow \infty$ ), it has worse resolution characteristics by the **Rayleigh** criterion than the rest of methods. But having a real finite size sample, when fine effects of “**sticking together**” breakdown due to estimation errors, their advantages compared with the **Capon** method disappear and the latter appears to be the most “robust” in these conditions (Section VII).

5. New kinds of “superresolving” **DoA** estimation methods with essentially better statistical characteristics are proposed. It is shown that on their basis, already with small effective sample sizes  $\delta = N - M \geq 0$ , the sources are resolvable by the **Rayleigh** criterion with such a probability that on the basis of known methods is either provided given much larger sample sizes  $\delta \gg 1$  or not provided at all.

The possibility of aggregate (“bank”) of proposed **NES** methods realization on the unified structurally algorithmic basis of adaptive lattice filters (**ALF**) is noted. The corresponding “**ALF-bank**” is signifi-

cantly more robust to impact of various decorrelating factors than “banks” of ES methods of MUSIC type. Therefore namely the “ALF-bank” is most suitable for practical realization of Gershman’s idea [12, 43 – 46] about direction finding using high-resolution bearing estimators of various types (Section VIII).

## References

- [1] S.L. Marple, Jr., Digital Spectral Analysis with Applications, Prentice Hall, 1987.
- [2] S. Haykin, J. Litva, T.J. Shepherd (Eds.), Radar Array Processing, Springer-Verlag, Berlin, 1993.
- [3] P. Stoica, R.L. Moses, Introduction to Spectral Analysis, Prentice Hall, Upper Saddle River, NJ, 1997.
- [4] H. Krim, M. Viberg, Two decades of array signal processing research: the parametric approach, IEEE Signal Processing Mag., vol. 13, no. 4 (1996) 67–94.
- [5] V.V. Drogalin, V.I. Merkulov, V.A. Rodzivilov et al., Algorithms for estimation of radiation sources angular coordinates based on spectral analysis methods, Radiolocation and Radiometry, 1 (1999) 52–68, in Russian.
- [6] J. Munier, G.Y. Delisle, Spatial analysis in passive listening using adaptive techniques, IEEE Proc., vol. 75, no. 11 (1987) 1458–1471.
- [7] P. Stoica, A. Nehorai, MUSIC, maximum likelihood, and Cramer-Rao bound, IEEE Trans. Acoust., Speech, Signal Process., vol. 37, no. 5 (1989) 720–741.
- [8] P. Stoica, A. Nehorai, MUSIC, maximum likelihood, and Cramer-Rao bound: further results and comparisons, IEEE Trans. Acoust., Speech, Signal Process., vol. 38, no. 12 (1990) 2140–2150.
- [9] P. Stoica, A. Nehorai, Performance study of conditional and unconditional direction-of-arrival estimation, IEEE Trans. Acoust., Speech, Signal Process., vol. 38, no. 10 (1990) 1783–1795.
- [10] P. Stoica, K.C. Sharman, Novel eigenanalysis method for direction estimation, IEE Proc. F Radar and Signal Process., vol. 137, no. 1 (1990) 19–26.
- [11] D.I. Lekhovitskiy, P.M. Flexer, D.V. Atamanskiy, I.G. Kirillov, “Statistical analysis of some “superresolution” noise direction finding methods in array antenna at finite number of snapshots,” Antennas, no. 2 (45), pp. 23–39, 2000, in Russian.
- [12] A.B. Gershman, Direction finding using high-resolution bearing estimators of various type, Radiotechn. and Electron., vol. 40, no. 6 (1995) 918–924.
- [13] A.B. Gershman, P. Stoica, On unitary and forward-backward MODE, vol. 9, no. 2, (1999) 67–75.
- [14] O.P. Cheremisin, Efficiency of adaptive methods for interference direction finding, Radiotechniques and Electronics, vol. 34, no. 9, (1989) 1850–1861, in Russian.
- [15] D.I. Lekhovitskiy, P.M. Flekser, Statistical analysis of quasi-harmonic spectral estimation resolution with Capon’s method, Proc. Int. Sci. and Tech. Conf. “Modern Radiolocation”, Kyiv, Ukraine, vol. 1, (1994) 66–71, 1994, in Russian.
- [16] D.I. Lekhovitskiy, P.M. Flekser, Statistical analysis of the resolution of adaptive spectral estimation algorithms, Abstracts of Int. Sci. and Tech. Conf. “Modern Radiolocation”, Kyiv, Ukraine, vol. 1, (1994) 134, in Russian.
- [17] D.I. Lekhovitskiy, S.B. Milovanov, V.M. Pishchukhin, P.M. Flekser, Modified Capon algorithm for problems of the harmonic spectral analysis of space-time random signals, Abstracts of the 5th all-Union school-seminar “Design of automated systems for compound objects control and driving”, Tuapse, (1992), in Russian.
- [18] Ya.D. Shirman, V.N. Manzhos, D.I. Lekhovitskiy, Some stages of development and problems of the radar signals resolution theory and technique, Radiotechniques, no. 1, (1997) 31–42, in Russian.
- [19] D.I. Lekhovitskiy, D.V. Atamanskiy, I.G. Kirillov, P.M. Flexer, Problems and new results of spectral estimation and antenna arrays superresolution techniques, Proc. of the 3rd Int. Conf. Antenna Theory and Techniques, Sevastopol, Ukraine, (1999) 62–68.
- [20] Ya.D. Shirman, Theory of useful signal detection against the background of Gaussian noise and the arbitrary number of interfering signals with random amplitudes and initial phases, Radiotechniques and Electronics, vol. 4, no. 12, (1959) in Russian.
- [21] Ya.D. Shirman, Statistical analysis of optimal resolution, Radiotechniques and Electronics, vol. 6, no. 8, (1961) 1232, in Russian.
- [22] J. Capon, N.R. Goodman, Probability distributions for estimators of the frequency-wavenumber spectrum, IEEE Proc., vol. 58, no. 10 (1970) 1785–1786.
- [23] L.E. Brennan, I.S. Reed, An adaptive array signal processing algorithm for communications, IEEE Trans. Aerosp. Electron. Syst., vol. 18, no. 1 (1982) 124–130.
- [24] J.P. Burg, Maximum entropy spectral analysis, paper presented at the 37<sup>th</sup> Annual International Meeting, Soc. of Explor. Geophys., Oklahoma City, Okla., (1967).
- [25] V.V. Karavaev, V.S. Molodtsov, Accuracy characteristics of the superresolving antenna, Radiotechniques and Electronics, vol. 32, no. 1, (1987) 22–26, in Russian.
- [26] V.T. Yermolaev, K.V. Rodyushkin, The distribution function of maximum eigenvalue of sample correlation matrix of internal noise of antenna array elements, Izvestiya vuzov. Radiophysics, vol. 42, no. 5, (1999) 494–500, in Russian.
- [27] A.B. Gershman, V.T. Yermolaev, Interconnection between spectral estimates of maximum entropy and “thermal noise”, Radiotechniques, no. 9, (1988) 39, in Russian.
- [28] D.I. Lekhovitskiy, On the theory of adaptive signal processing in systems with central symmetry of receiving channels, Radiotechniques, no. 100, pp. 140–158, 1996, in Russian.
- [29] D.R. Brillinger, Time Series: Data Analysis and Theory, Holden-Day, Inc., San Francisco, 1981.
- [30] N.A.J. Hastings, J.B. Peacock, Statistical Distributions: A Handbook for Students and Practitioners, Butterworth, London, 1975.
- [31] A.P. Prudnikov, Yu.A. Brychkov, O.I. Marichev, Integrals and Series. Additional Chapters, Nauka, Moscow, 1986, in Russian.
- [32] J.P. Burg, The relationship between maximum entropy and maximum likelihood spectra, Geophysics, vol. 37 (1972) 375–376.
- [33] D.I. Lekhovitskiy, D.V. Atamanskiy, I.G. Kirillov, Kinds of “superresolving” space-time spectrum analyzers of random signals on the basis of whitening adaptive lattice filters, Antennas, no. 2 (45), (2000) 40–54, in Russian.
- [34] Ya.D. Shirman, Signal Resolution and Compression, Soviet Radio, Moscow, 1974, in Russian.
- [35] Ya.D. Shirman (Ed.), Radioelectronic Systems: Fundamentals of Construction and the Theory, Handbook, 2nd ed., Radiotechniques, Moscow, 2007, in Russian.



- [36] J. Capon, High-resolution frequency-wavenumber spectrum analysis, IEEE Proc., vol. 57, no. 8 (1969) 1408–1418.
- [37] B. Friedlander, Lattice filters for adaptive processing, IEEE Proc., vol. 70, no. 8 (1982) 829–867.
- [38] C.F.N. Cowan, P.M. Grant (Eds.), Adaptive filters, Prentice Hall, Englewood Cliffs, N.J., 1985.
- [39] D.I. Lekhovyt'skiy, Generalized Levinson's algorithm and universal lattice filters, Radiophysics, vol. 35, no. 9–10 (1992) 790–808, in Russian.
- [40] D.I. Lekhovyt'skiy, thirty years experience in development of adaptive lattice filters theory, techniques and testing in Kharkiv, Proc. of the VIII Int. Conf. Antenna Theory and Techniques, Kyiv, Ukraine, (2011) 51–56.
- [41] M.F. Bondarenko, D.I. Lekhovyt'skiy, Combined direction finders of point noise radiation sources in AA based on adaptive lattice filters, Proc. of the First IEEE Int. Workshop on Computational Advances in Multi-Sensor Adaptive Processing, Puerto Vallarta, Jalisco, Mexico, (2005).
- [42] D.I. Lekhovyt'skiy, D.V. Atamanskiy, V.V. Dzhus, F.F. Mysik, Comparison of different type combined direction-finders resolutions in receive systems with non-identical channels, Antennas, no. 12 (79) (2003) 9–15, in Russian.
- [43] A.B. Gershman, High-resolution direction finding using eigendecomposition based estimators and joint estimation strategy, Electronics Letters, vol. 27 (1991) 2308–2309.
- [44] A.B. Gershman, Pseudo-randomly generated estimator banks: a new tool for improving the threshold performance of direction finding, IEEE Trans. Signal Process., vol. SP-46 (1998) 1351–1364.
- [45] A.B. Gershman, J.F. Böhme, Pseudorandomly generated estimator banks: a new resampling scheme for improving the threshold performance of second and higher-order direction finding methods, Proc. of the 2nd Int. Conf. on Antenna Theory and Techniques, Kyiv, Ukraine, (1997).
- [46] A.B. Gershman, Direction finding using beamspace root estimator banks, IEEE Trans. Signal Process., vol. SP-46 (1998) 3131–3135.
- [47] R.J. Muirhead, Aspects of Multivariate Statistical Theory, Wiley, New York, 1982.
- [48] C.D. Richmond, Capon algorithm mean squared error threshold SNR prediction and probability of resolution, IEEE Tran. Signal Process., vol. 53, no. 8 (2005) 2748–2764.
- [49] D.I. Lekhovyt'skiy, Y.S. Shifrin, and D.V. Atamanskiy, “Rapidly convergent “superresolving” direction finders of noise radiation sources in adaptive arrays,” Proc. of the 9th International Conference on Antenna Theory and Techniques, ICATT 2013, pp. 28–33, 2013
- [50] D.I. Lekhovyt'skiy and Y.S. Shifrin, “Statistical analysis of “superresolving” methods for direction-of-arrival estimation of noise radiation sources under finite size of training sample,” Signal Processing, vol. 93, no. 12, pp. 3382–3399, 2013.

Поступила в редколлегию 10.02.2015



**David I. Lekhovyt'skiy**, Doctor of Technical Science Professor, Chief researcher in the Kharkiv National University of Radio Electronics. Research interests are in adaptive space-time signal processing in different information systems.



**Yakov S. Shifrin**, Doctor of Technical Science Professor, Chief researcher in the Kharkiv National University of Radio Electronics. Research interests are radiophysics and applied electrodynamics.

УДК 621.396.965

**Швидкодіючі «надрозділяючі» методи оцінювання напрямків джерел шумових випромінювань в адаптивних АР / Д. І. Леховицький, Я. С. Шифрін // Прикладна радіоелектроніка: наук.-техн. журнал. – 2015. – Т. 14. – № 1. – С. 7–23.**

Порівнюється ефективність деяких «надрозділяючих» методів оцінювання в АР просторового спектра гаусівських шумових випромінювань при кінцевому обсязі навчаючої вибірки в максимально правдоподібній оцінці їх кореляційних матриць. Порівняння базується на аналізі точних або емпіричних законів розподілу випадкових параметрів, що визначають роздільну здатність відповідних методів за статистичними та нестатистичними критеріями. Показано істотну відмінність цих законів для різних методів, у зв'язку з якою висновки, які базуються на аналізі асимптотичних властивостей цих методів, можуть змінитися на протилежні в реальних умовах вибірок малого обсягу. Встановлюються причини цих відмінностей та, впливаючи з їх аналізу, можливості підвищення «швидкодії» адаптивних методів пеленгації джерел шумових випромінювань в АР.

**Ключові слова:** оцінювання напрямку поширення, «надрозділяючий» просторово-часовий спектральний аналіз, швидкодія, статистичний аналіз, розділення, вибірка обмеженого обсягу, адаптивний решітчастий фільтр.

Лл.: 11. Бібліогр.: 50 найм.

УДК 621.396.965

**Быстродействующие «сверхразрешающие» методы оценивания направлений источников шумовых излучений в адаптивных АР / Д. И. Леховицкий, Я. С. Шифрин // Прикладная радиоэлектроника: науч.-техн. журнал. – 2015. – Т. 14. – № 1. – С. 7–23.**

Сравнивается эффективность ряда «сверхразрешающих» методов оценивания в АР пространственного спектра гауссовских шумовых излучений при конечном объеме обучающей выборки в максимально правдоподобных оценках их корреляционных матриц. Сравнение базируется на анализе точных или эмпирических законов распределения случайных параметров, определяющих разрешающую способность соответствующих методов по статистическим и нестатистическим критериям. Показаны существенные различия этих законов, в силу которых выводы о сравнительных достоинствах различных методов, основанные на анализе их асимптотических свойств, могут меняться на противоположные в реальных условиях выборок малого объема. Устанавливаются причины этих отличий и вытекающие из их анализа возможности повышения «быстродействия» адаптивных методов пеленгации источников шумовых излучений в АР.

**Ключевые слова:** оценивание направления прихода, «сверхразрешающий» пространственно-временной спектральный анализ, быстродействие, статистический анализ, разрешение, выборка конечного объема, адаптивный решетчатый фильтр.

Рис.: 11. Библиогр. : 50 назв.